Determination of bio-accessible amounts of metal trace elements in baby food using *In vitro* artificial digestion.

Carl Marcus Andersson
Spring 2022

Bachelor thesis: 30 hp
Subject area: Chemistry
School of Science and Technology, Örebro university.
Supervisor: Michaela Zeiner
Examiner: Stefan Karlsson

ABSTRACT

Prefabricated baby food is under strict EU legislation by Commission Regulation (EC) 1881/2006 *Setting maximum levels for certain contaminants in foodstuffs* regarding the maximum allowed content of potentially harmful elements. For potentially toxic trace elements the regulated maximum content is regulated for lead, cadmium, mercury, inorganic tin, inorganic arsenic, cesium, copper and manganese. The Swedish national food agency (Livsmedelsverket) conducts chemical analyses of the regulated elements by full microwave acid digestion followed by Inductively Coupled Plasma Mass Spectrometry (ICP-MS) analysis. In this study a simple artificial *in vitro* digestion method was developed using a commercially available enzyme supplement and optimized to determine the bio-accessible amount of eight potentially harmful metal trace elements that are associated with modern electronics (lithium, vanadium, cobalt, nickel, arsenic, selenium, cadmium and lead) in five prefabricated baby meals from the Swedish market by well-established manufacturers. The results were compared to the total mass content as well as the regulated limits and toxicological literature data. The samples had analyte dry mass contents that were extractable by the developed *in vitro* method that ranged from 0.0314 $\mu g\ g^{-1}$ to 0.0691 $\mu g\ g^{-1}$ for lithium, $9.42*10^{-5}$ $\mu g\ g^{-1}$ to 0.0152 $\mu g\ g^{-1}$ for vanadium, $6.61*10^{-3}$ $\mu g\ g^{-1}$ to $30.9*10^{-3}$ $\mu g\ g^{-1}$ for cobalt, 0.0599 $\mu g\ g^{-1}$ to 0.194 $\mu g\ g^{-1}$ for nickel, $4.54*10^{-4}$ $\mu g\ g^{-1}$ to 0.0431 $\mu g\ g^{-1}$ for arsenic, $8.87*10^{-4}$ $\mu g\ g^{-1}$ to $9.85*10^{-3}$ $\mu g\ g^{-1}$ for cadmium and $1.24*10^{-3}$ $\mu g\ g^{-1}$ to 0.0232 $\mu g\ g^{-1}$ for lead. Selenium was not detected in any of the samples. None of the samples were found to contain toxic levels of any of the quantified elements. Comparisons and paired t-tests of recoveries between the *in vitro* digestion and control procedures consisting of digestion solutions that exclude either enzymes, pH adjustment or both suggested that lithium, cobalt and cadmium were protein bound and that the digestion enzymes used had a statistically significant effected on the recovery. With further optimization and more extensive comparison to reference data the method could potentially be established as a simple and affordable alternative to more elaborate methods for screening or small scale analysis of the bio-accessible fraction of metal trace elements in food.

Keywords: Food, toxic metals, children, bio-accumulation, artificial digestion, ICP-MS

TABLE OF CONTENTS

1. INTRODUCTION AND THEORY

1.1 Background and previous studies

Prefabricated food items for young children is a large market business that in Sweden had an estimated annual value of up to 143 million euros in 2017 (Luan Gjokaj, 2017).

In Sweden and other countries in the European Union, commercial food products for children are under strict regulation to keep levels of potentially harmful constituents below certain limits. These limits are established by the Commission Regulation (EC) No. 1881/2006 *Setting maximum levels for certain contaminants in foodstuffs* (*(EC) No 1881/2006*, 2006). In these regulations a few trace elements, including Pb, Cd, inorganic Sn, Hg and As, are provided with specific set limits for baby food that must be followed for in order to be allowed to be sold (table 1). As a comparison the maximum allowed lead content in food types not specifically targeted to children ranges from 0.020 mg kg^{-1} in raw milk to 1.5 mg kg^{-1} in bivalve mollusks. The maximum allowed cadmium levels range from 0.050 mg kg^{-1} in meat and fish to 1.0 mg kg^{-1} in bovine kidney, bivalve mollusks and cephalopods. Inorganic arsenic allowed content ranges from 0.20 mg kg^{-1} in non-parboiled milled rice to 0.30 mg kg^{-1} in Rice-waffles, -wafers, -crackers and -cakes. Baby food items are controlled regularly for these elements and in Sweden the national food agency (Livsmedelsverket) conducts regular investigations on the subject.

Table 1. Regulated maximum content of some trace elements in baby food items.

Element	Content limit (in marketed product)
Lead	0.050 µg g^{-1}
Cadmium	0.040 µg g^{-1}
Mercury	0.05 µg g^{-1}
Tin (inorganic)	50 µg g^{-1}
Arsenic (inorganic)	0.10 µg g^{-1}
Cesium 137	300 Bq kg^{-1}
Iron	3 mg per 100 kcal
Copper	40 µg per 100 kcal
Manganese	0.6 mg per 100 kcal

However, the limits set by EU legislation, as well as the analytical investigations, almost exclusively focus on the total content of these elements without regard taken to their bio-accessibility to young children. Bio-accessibility is defined as the amount of a compound that is available to be absorbed into the body through the gastro-intestinal tract (Charis Galanakis, 2017). In a study conducted in 2017 by the Swedish national food agency (Livsmedelsverket, 2018) the amounts of regulated trace elements in 35 baby food products (oatmeal and rice based) were all found to be below the regulated limits and also lower than in previous studies which was speculated to be a result of increasing awareness and subsequent quality control by the producers to keep within regulation. It was also found that the amounts varied depending on the raw

materials used. Wheat is known to bio-accumulate all regulated trace elements (Guo *et al.*, 2018) while beef bio-accumulates cadmium, zinc and lead to varying degrees (Kasozi *et al.*, 2021).

1.2 Analytes of interest

1.2.1 General information

Metal trace elements occur naturally in the earth's crust in the form of mineral species, and human activities have increased their content in the environment over the last decades. They can be assumed to increase further as production of electronic products goes up and becomes more readily available to a larger part of the global population. As the elements are leached from electronics into the environment they can end up in soil and water near farms and fields that produce animals and food crops for consumption.

Toxic metal trace elements have often been colloquially referred to as "heavy metals" due to the fact that many of them have densities of at least 5 g/cm^3, but since many lighter metals have been found to demonstrate similar toxic properties the term has little scientific meaning (Duffus, 2002) and is being phased out. In this study the term Metal Trace Element (MTE) will instead be used which also covers metalloids such as arsenic and selenium (Bocquet *et al.*, 2021). The MTEs found in food products that are also regulated by EU legislation are few and have not been changed since they were implemented. It could therefore be of interest to determine some potentially harmful MTEs that are associated with modern electronics such as lithium, cobalt, vanadium and nickel. These are for instance used in the production of rechargeable batteries, LCD displays, circuit boards and other components that can be found in everyday electronics such as smartphones and laptops, whose presence have increased substantially over the previous decades (Reimer, 2012).

With these points in mind the target MTEs chosen for this study were lithium (Li), vanadium (V), cobalt (Co), nickel (Ni), arsenic (As), selenium (Se), cadmium (Cd) and lead (Pb). This encompasses As, Cd and Pb which have regulated content limits, as well as Li, V, Co, Ni and Se that are elements with known health risks that are common in modern electronics (Nimpuno *et al.*, 2011). Li, V, Co and Se are trace elements that are essential to life (E.g. Co(II) is a component of vitamin B12) while Cd, Ni, As and Pb are non-essential and the toxic threshold concentrations for these are much lower (Bansal and Asthana, 2018).

1.2.2 Speciation, bio-accumulation and health risks related to MTEs

Arsenic, cadmium and lead all have extensive industrial uses and commonality in electronics which help propagate their contamination of crops and animals for human consumption, combined with high toxicity that can be both acute and chronic it makes them the highest risk factors of the MTEs of interest (Baird and Cann, 2012). In their ionic forms (Pb^{2+}, Cd^{2+} and As^{3+}) they readily form stable protein compounds with toxic properties (Engwa *et al.*, 2019). The major pathway to human exposure of MTEs is from industrial-/mining-sites ⟶ atmosphere ⟶ soil ⟶ water ⟶ plants/crops ⟶ humans (Khan *et al.*, 2015).

In ionic form some MTEs such as Cd^{2+}, and to some extent Pb^{2+}, are known to bind to the thiol groups on chelating agents (Bjørklund *et al.*, 2019) and can generate conformational changes to enzymes inhibiting their functions (Luch, 2010). Examples are selenomethionine and cadmium(II) complex formation via the terminal amino group on all types of amino acids

(Sóvágó and Várnagy, 2013). Cadmium binds to the protein family metallothionein that contains several thiol groups and are found in liver and kidney tissue and is known to promote apoptosis. Lead mostly accumulates in the body as phosphate salt ($Pb_3(PO_4)_2$) bound to bone, hair and teeth. Both lead and cadmium can bind to blood cells and be distributed to organs such as the liver and kidneys. Arsenic is most toxic in inorganic arsenite and arsenate forms and accumulates in several tissues including heart, lung and muscles. Several MTEs can generate free radicals that can cause oxidative stress and molecular damage to enzymes, proteins, lipids and DNA. One example is ionic cobalt (Co^{2+}) that via decomposition of H_2O_2 can generate the anion radical superoxide that can cause oxidative stress and trigger apoptosis. Cobalt have been reported to bioaccumulate in wheat with bioconcentration factors (BCF) ranging between 0.441 to 0.926 (Ejaz *et al.*, 2022). Vanadium, Co, Ni and Cd are known carcinogens that can regulate transcription factors and control gene expressions (Engwa *et al.*, 2019). Vanadium(V) in blood is readily reduced to vanadium(IV) that can bind to proteins and be distributed to remote organs (Crans *et al.*, 2004). It can also speciate as oxyanions such as vanadyl and vanadate and can bind to the blood transferring protein transferrin. V_2O_5 is amphoteric and will form VO_2^+ in acidic environments (Rehder, 2013). Most common lithium species are water soluble (LiOH, LiCl and Li_2CO_3).The major source of digested lithium intake to humans is from plants whose uptake mechanism is not fully understood yet but due to it being a group 1 element it has similar properties to Na^+ and K^+ and is theorized to have a water-plant pathway in ionic form. Lithium is not known to be bio-accumulative in animals (Shahzad *et al.*, 2016).

Most MTEs of interest to this project do not have EU regulated maximum content levels in baby food and they lack general regulated intake levels as well due to absence of dose-response data. But most have estimated average dietary intake levels or known toxic doses that can be used for rough comparisons. Selenium has a daily intake limit of 60 µg/day for children aged 1-3. Vanadium has no defined tolerable upper intake level but studies have shown that normal intake for an adult human is ~10-20 µg/day and doses of ~20000 µg/day have been reported to have adverse effects. Nickel has no defined daily upper intake level but normal dietary intake in adult humans is estimated to be 2.5 µg/day/kg BW and the lowest dose to show adverse effects in rats is 1250 µg/day/kg BW. Cobalt does not have a defined recommended upper intake level but has an estimated average daily uptake by adult humans of ~5-8 µg/day. The values were gathered from a report by the European Food Safety Authority released in 2006 (EFSA, 2006) that was based on figures from EU Regulation (EC) No 178/2002. No reported toxic oral intake level for Li could be found.

1.2.3 Proteins and metals

Proteins are made of amino acids that are amphoteric and can have either negative, neutral or positive net charge depending on the pH of their environment. At pH <6 the majority of amino acids are either neutral (As Zwitterions) or positively charged. As Zwitterion both terminals are charged but balances each other out (figure 2) to a net neutral.

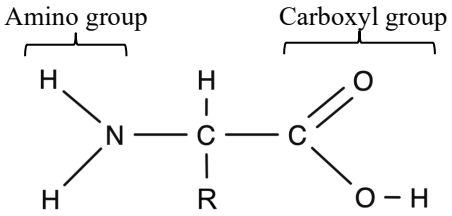

Figure 1. General amino acid structure. (drawn in molview.org)

The two major functional groups found in amino acids are the amino group (R-NH_2) and carboxyl group (R-COOH) which are present in all amino acids (figure 1). In both neutral and low pH states the amino group is protonated and positively charged and can bind to negatively charged ions.

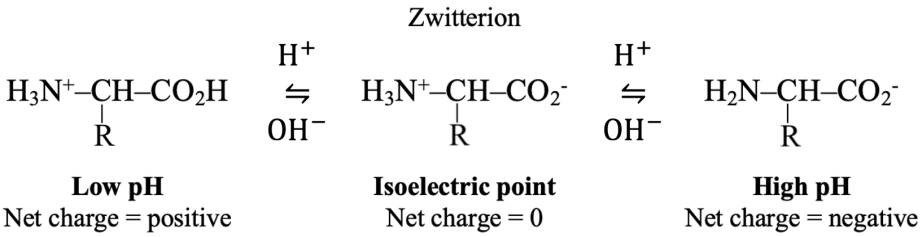

Figure 2. Charge states of amino acids in different pH.

Amino acid side chains containing functional groups are affected by pH by the same principle as shown in figure 2 and protonate/deprotonate at different pH-values. As the majority of amino acids are likely to be positively charged in the acidic environment of the samples, anionic species of the analytes are more likely to bind to them while species that are positively charged should be dissolved in the aqueous phase (Petrucci *et al.*, 2017).

1.3 Main human digestive enzymes

The human digestive system can be divided into three main parts the salivary, gastric and intestinal systems. The main constituents of human gastric secretion fluid is water, hydrochloric acid, salts (NaCl, KCl) and enzymes, with amylase, pepsin and human gastric lipase (HGL) as the predominant ones. The intestinal secretion fluid contains water, salts (NaCl, KCl, $NaHCO_3$ and $CaCl_2$), bile salts and the enzymes pancreatic lipase and trypsin. In children under the age of 12 months these systems are not yet fully developed and the composition ratios between the constituents are different compared to those of adults and therefore the digestion of food is not as complete (Bourlieu *et al.*, 2014). MTEs that bind strongly to matrix components that cannot be fully digested could therefore hypothetically pass through the body without becoming bio-accessible, and in turn decrease the potential extent of harm they can cause.

1.4 Acid digestion

To determine the ratio between the bio-accessible fraction and the total amount of MTEs in the samples, a full acid digestion was performed to quantify the total content. To do this purified (sub-boil distillation) HNO_3 was used to digest the samples. It is a strong oxidizing agent that is known to readily dissolve most metals in most biological matrices. It does not result in insoluble

salts forming with the MTEs and hence does not introduce unnecessary interferences during analysis. HNO_3 does not fully decompose fat and might result in charring of combustible materials if overloaded but it's generally a suitable digestion reagent in trace element analysis using ICP-MS and MP-AES (Holland, 2014).

1.5 Reference *in vitro* model

To determine the bio-accessible fraction of the analytes in the food samples, a sequential *in vitro* digestion model was developed. The method was based on the previous work by Ménard et al. from 2018 where they developed a static *in vitro* digestion method for liquid infant formula based on gastro-intestinal parameters of newborns and 28 days old infants (Ménard *et al.*, 2018). Their method was in turn based on data from an earlier study on specificity of infant digestive conditions (Bourlieu *et al.*, 2014). They found that the proteolytic and lipolytic kinetics differed based on the physiological stage of the child with pH and enzyme levels being the two main factors. The digestive systems of young children are not yet fully developed and during the first months after birth they are adapted to pass and digest primarily breast milk. As a result of ingesting breast milk without chewing the salivatory enzymes, mainly amylase, have a negligible impact on the digestion. The pH of the gastric and intestinal secretion fluids are higher than in adults and the enzymatic activities are lower. The liquid infant formula they used had an measured protein ratio of *w/w* 30:70, lipid content of 43% and 7.5% hydrocarbons.

Since amylase was assumed not to impact the digestion, an oral phase was not included in their model and a two part sequential digestion composed of a gastric and an intestinal phase was made. The gastric phase digestion used a simulated gastric fluid (SGF) that was made of porcine pepsin and lipase from Sigma Aldrich, rabbit gastric extract, NaCl and KCl. The pH was set to 5.3 and the temperature 37°C with a gastric digestion time of 60 min in accordance to extrapolated data from the study by Bourlieu *et al.* (2014). Between the gastric and intestinal phases the pH was adjusted to 7 in order to keep the enzymes from further digesting the samples during the transferring process. The intestinal phase used a simulated intestinal fluid (SIF) that was made of porcine pancreatin, bile salts, NaCl, KCl, $NaHCO_3$ and $CaCl_2$. The sample containing the SGF was combined with the SIF and set to pH 6.6 before being incubated at 37°C for 60 min. The concentrations of the SGF and SIF constituents as well as the duration and temperature was based on conditions in infant gastric aspirates at the gastric half-emptying time ($GE_{1/2}$) since that was assumed to be more representative than at the final time point. The mean weight of a one-month-old was used when they calculating the per body weight amounts of enzyme and salts (Ménard *et al.*, 2018).

Particle size, protein, lipids and free fatty acids where analyzed at 5, 15, 30 and 60 minutes using a multitude of instrumental analysis tools such as Confocal Laser Scanning Microscopy (CLSM), Laser Light Scattering with two laser sources (Mastersizer 2000), Aodium Dodecyl Sulfate–PolyAcrylamide Gel Electrophoresis (SDS-PAGE), Nuclear Magnetic Resonance (NMR), Gas Chromatography (GC) and Thin Layer Chromatography (TLC). In their proteolysis analysis of the residual protein throughout the gastric digestion phase they found that the residual casein in the samples decreased from ~50% at 5 minutes to ~10% at 60 minutes. The amount of residual β-lactoglobulin and α-lactalbumin at 5 minutes was ~90% and ~100% respectively, and ~80% and 90% respectively at 60 minutes (Ménard *et al.*, 2018).

1.6 Vegetable digestive supplement enzymes

This project focused on a simple method, and not to replicate the full procedure by Ménard *et al*. from 2018, so a commercially available enzyme supplement was purchased and the amount of added enzyme was set to correspond with the activity of gastric and pancreatic proteases (pepsin and trypsin). Protease was chosen due to the aforementioned speciation of the analytes in acidic environment. They are unlikely to be found in non-polar or less polar media such as adipose tissue.

2. AIM

The aim of the project was to develop a simple *in vitro* digestion method for determination of the bio-accessible fraction of potentially toxic MTEs in prefabricated food targeted at 6- to 12-month-old children.

Goals

- To determine the element specific total content and bio-accessible fraction extracted by the *in vitro* model.
- To compare the total content determined in the samples to the regulated limits set by EU for Pb, Cd, As.
- To determine the element specific ratio between total content and bio-accessible fraction from *in vitro* digestion.

3. MATERIALS AND METHOD

3.1 Quality assurance and quality control

Quality assurance included the use of procedural blanks for all methods. Six replicates and three blanks were used for each sample in the complete *in vitro* digestion and control samples, and six replicates for each sample and one blank for the complete HNO_3-digestion and water extractions. For the optimization runs three replicates per sample and one blank was used. For the ICP-MS a rhodium internal standard was used to minimize signal instability as well as an ICP multi-element standard solution (Merck VI) containing the elements of interest. To assure good sample variability four different batches from the respective five manufacturers were bought. All labware was of analytical grade and made of polypropylene (PP) except for the mortar and pestle used to crush the dried sample. When used more than once the PP labware was cleaned thoroughly in a 10% HNO_3 bath (≙ ~2.4 mol L^{-1}), the mortar and pestle was cleaned using DI water. Basic optimizations of the methods were performed by testing different dilution factors and reagent concentrations before conducting the final analyses. For quality control several statistical analyses were performed which are described in detail in the method section.

3.2 Sampling strategy and sample data

Prefabricated baby food 6+ months (pasta, vegetables and beef)

The sampling procedure consisted of buying one type of baby food (pasta Bolognese for children 6+ month-old) in four different batches from five major manufacturers established on the Swedish market (table 2). In addition, a home cooked meal of pasta Bolognese was prepared by emulating the average composition of the prefabricated meals. The total number of collected samples were n = 21 (5 manufacturers x4 batches + 1 home cooked meal).

Table 2. Sampled prefabricated baby food including specified ingredient percentages as well as fat and protein mass content (Samples 1-5).

Sample ID	Pasta %	Beef %	Tomato %	Carrot %	Combined vegetables %	Fat content (g/100 g)	Protein content (g/100 g)
Sample 1	29	5	32	30	-	2.5	2.3
Sample 2	17	10	-	-	67	3.0	3.4
Sample 3	7.5	8	-	-	57	2.5	2.8
Sample 4	28	8	3	8	-	2.4	3.1
Sample 5	26.3	8.9	9	22.2	-	2.2	3.5

3.3 Home cooked pasta Bolognese sample

3.3.1 Ingredients

The home cooked pasta Bolognese (sample 6) was prepared by matching the ingredient ratios of the prefabricated meals using the mean values of the percentages of each ingredient stated on the jars. All ingredients used for the home cooked meal were organic and from well-established Swedish manufacturers (table 3).

Table 3. Ingredients in home cooked pasta Bolognese (sample 6)

Ingredient	Best before date	Details	Percent of meal (%)
Spaghetti	03-10-2024	Durum wheat	22
Ground beef	02-02-2022	fat <15 %	8
Carrots	-	Package day: 024 Time: 11:08 Field: Engfältet, 142-1	30
Rapeseed oil	21-12-2022	-	< 0.5
Pasta sauce	12-10-2023	Crushed tomatoes 70 %, Tomato purée, Basil 1 %, olive oil, onion, salt and garlic.	30
Tap water	-	-	10

3.3.2 Method of preparation

The pasta was boiled in a stainless steel pot for 15 minutes (8 minutes longer than specified on the packaging) to reach a soft consistency comparable to the prefabricated meals. The beef was fried in a cast iron frying pan using organic rapeseed oil until well done. The carrots were boiled until they were soft and could be crushed without much force using a fork. All ingredients were cooled to room temperature and mixed into a consistency comparable to the prefabricated samples using a household stick mixer. Tap water and ordinary household items were used to expose the food to trace elements found in homes. Total mass of the prepared meal was approximately 300 g.

3.4 Drying and determination of dry mass

The samples were weighed in 50 mL PP-tubes from Sarstedt using a Sartorius BP 221 S analytical scale. The samples were then dried in an oven at 105℃ for ~140 hours and then weighed at 1 hour intervals until constant mass was reached. Constant mass was decided to be reached when a decrease in <0.05 g between hourly controls was observed. The dried sample was crushed using a Haldenwanger™ glazed mortar and pestle made from optimized laboratory porcelain, it was then transferred to a 50 mL PP-tube using a disposable plastic spoon. Between samples the spoons were discarded and the mortar and pestle were cleaned from debris. The water content of the wet products were calculated using Microsoft Excel (version 16.57) and ranged from 83.8% - 87.1% depending on manufacturer (See table 4).

Table 4. Wet and dry mass (g), water content (% *w/w*) and wet/dry factor of samples 1 - 6.

Sample ID	Sample wet mass	Sample dry mass	Water content	Wet/dry factor
Sample 1	26.0	3.34	87.1%	7.78
Sample 2	28.2	4.36	84.5%	6.47
Sample 3	27.0	3.89	85.5%	6.89
Sample 4	25.6	4.15	83.8%	6.17
Sample 5	25.5	3.76	85.3%	6.80
Sample 6	27.9	3.96	85.8%	7.04

3.5 Acid Digestion

3.5.1 Acid digestion method optimization

To determine the optimal composition and concentration for an acidic digestive solution that could be used to digest the samples and produce the highest recovery as well as most stable ICP-MS signals for all analytes of interest, two setups were performed using H_2O_2 and HNO_3.

3.5.2 H_2O_2 setup

Approximately 0.30 g of dry sample (sample 1) weighed to the nearest 0.1 mg was put to a 50 mL PP-tube. Fifty mL of 30% H_2O_2 was then carefully added using an auto-pipette. Only a very minor reaction was noticed with minimal foam formation on the surface and a slight coloration of the added acid. A procedural blank was prepared in tandem. The solution was left to react for approximately 60 hours. After reacting with the acid the solution had changed color from dark brown to pale yellow. The solution and blank were put in a water bath at 60°C for 5 h to increase the reaction rate. After removing the solution from the water bath a distinct amount of suspended matter was still visible in the solution and oil/fat residue was resting on the surface of the solution and walls of the tube. Since the sample had not dissolved sufficiently it was decided not to analyze the solution further.

3.5.3 HNO_3 concentration setup

Dry sample (sample 1) was prepared in three sets of triplicates with different concentrations consisting of 20%, 60% or 100% concentrated HNO_3 solution (≙ ~2.8 mol L^{-1}, ~8.4 mol L^{-1} and ~14 mol L^{-1}). Approximately 0.20 g of dry sample weighed to the nearest 0.1 mg was transferred to three 50 mL PP-tubes and then mixed carefully with 5.0 mL HNO_3 of each concentration respectively. No immediate reaction was observed when adding the acid, but a slight fogging of the inner wall of the tubes slowly formed. The samples were then put in a heated water bath at the solutions boiling point (90°C) and checked periodically (Liem-Nguyen *et al.*, 2020). During the heating process the solid matter could be seen producing gas and release vapor. After 2.5 h the vapor release had stopped, the solid matter had been digested and the solutions were yellow (due to HNO_3 decomposing into NO_2 when heated which tints the solution yellow) and clear, i.e. no solid matter could be discerned by the naked eye. The solutions were cooled to room temperature and diluted to 50 mL using DI water and then filtered through 0.2 µm syringe filters (polypropylene, VWR brand). The filtered solutions were further diluted by a factor of 2.5 and 25 µL of concentrated HNO_3-solution was added. The prepared solutions were analyzed using ICP-MS (see settings in table 6).

3.5.4 Complete HNO_3 digestion and water leaching procedure

A complete digestion of all the samples (1-6) and enzyme supplement were performed based on the results from the previous optimization to determine the maximum extractable mass content that could be used to calculate an approximate ratio between contents from the *in vitro* digestion, as well as to determine the elemental composition of the rice bran filler agent of the enzyme supplement capsules. All samples were prepared as six replicates and one procedural blank. One set of six replicates using sample 1 was prepared using only 5.0 mL of DI water instead of 60% HNO_3 solution for a complementary water leaching procedure, using the same method as with the HNO_3 solutions described below. Approximately 0.20 g of each sample weighed to the nearest 0.1 mg (1-6) was transferred to 50 mL PP-tubes and 5.00 mL of 60% HNO_3 solution were carefully added using an auto-pipette. No immediate reaction was observed. The solutions were heated using a water bath at 90°C. After 2.5 h the solutions were removed and had become visually clear and yellow. DI water was added up to the 50 mL mark of the PP-tube in each solution, which were then filtered through 0.2 µm syringe filters. 4.00 mL of the filtered solutions were transferred to 15 mL PP-tubes using an auto-pipette and diluted to the 10 mL mark on the PP-tube with DI water using plastic pipettes for a total dilution factor of 2.5. To each solution 25 µL of concentrated HNO_3, and 10 µL of a 1 mg L^{-1} rhodium IS per mL solution for a final concentration of 10 µg L^{-1} was added using an auto-pipette and the solutions were analyzed via ICP-MS.

3.6 *In Vitro* Digestion

3.6.1 Optimization procedures

3.6.1.1 Pooling samples

Preliminary ICP-MS analysis of different manufacturer batches showed that there was no significant difference ($p > 0.24$) between the achieved results for different batches. By averaging the standard deviation between each set of four batches it was found that there was only a mean relative standard deviation of <4.0%. The batches were therefore pooled and six replicates from each pooled sample were further prepared.

3.6.1.2 Dilution factor

The dilution factor for the *in vitro* samples was set to 50 based on mass content data from the complete HNO_3 digestion as well as the Na^+ and Cl^- in the artificial *in vitro* gastro-intestinal solutions (containing ~8040 mg L^{-1} NaCl, ~4450 mg L^{-1} $NaHCO_3$ and ~830 mg L^{-1} KCl). This reduces the risk of damaging the ICP-MS or lowering the efficacy of the plasma by overloading it with Na, while still trying to keep the analytes of interest above the instrumental LOQ.

3.6.2 *In vitro* digestion reference method modification

3.6.2.1 Simulated artificial digestive fluids

The compositions of the SGF and SIF solutions used in the *in vitro* digestion were based on the reference method (Ménard *et al.*, 2018) that was based on data from an earlier study (Bourlieu *et al.*, 2014). Both methods focused on newborn infants and 28-day-old babies, as well as liquid foods such as infant formula and natural breast milk. To better match a 6- to 12-month-old child's gastro-intestinal system and the consistency of semi-solid food, the following modifications were made:

3.6.2.2 Meal : simulated fluid ratios

The volume ratios of sample to simulated secretion fluids (SGF and SIF) were replicated without modification from the reference article (Ménard *et al.*, 2018) and can be seen in figure 3.

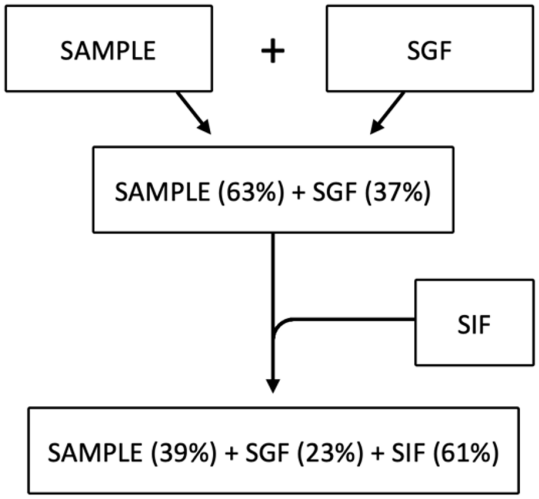

Figure 3. Flow chart of the general sample to simulated secretion fluid ratios of the sequential *in vitro* digestion described by Ménard et al. (Ménard *et al.*, 2018).

3.6.2.3 Calculating the gastric half emptying time ($GE_{1/2}$)

$GE_{1/2}$ for 6 month-old children was estimated to 84 minutes based on the $GE_{1/2}$ for infant formula (78 min) which is slower than for human milk (36 min) (Ewer *et al.*, 1994), and the fact that solid food has a longer $GE_{1/2}$ than liquid food with a factor of 1.14773 (Achour, *et al.*, 2001). The impact of this factor at 14.773 % was therefore halved to 7.3865 % giving a modified factor of 1.073865 so to represent a semi-solid food consistency that matches the samples used, resulting in formula (1).

$$78\ GE_{1/2} * 1.073865 = 83.76147\ GE_{1/2} \qquad (1)$$

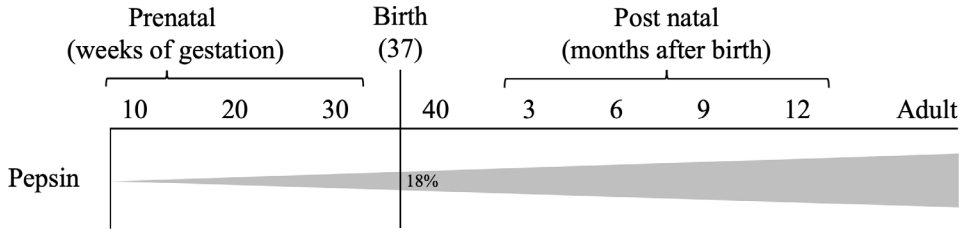

Figure 4. Pepsin activity levels at different ages (Bourlieu *et al.*, 2014).

3.6.2.4 Gastric and intestinal protease activities

Gastric pepsin activity was estimated to be 1.4 times higher at 6 months than at birth using extrapolation of data from the method by Bourlieu et al. (Bourlieu *et al.*, 2014; McClean and Weaver, 1993) as illustrated in figure 4. The average body mass of a 6-month-old child was determined to be 7.6 kg using growth standard charts (WHO, 2006). Resulting in calculations 2 and 3:

$$63\ \mathrm{U/mL/kg\ body\ weight} * 1.4 = 88.2\ \mathrm{U/mL} \quad (2)$$
$$88.2\ \mathrm{U/mL} * 7.6 = 670\ \mathrm{U/mL} \quad (3)$$

The mass of enzyme supplement to add to the simulated gastric and intestinal fluids was calculated by weighing the content of the enzyme supplement capsules and converting the combined enzymatic protease activities per gram from HUT to U/mL and matching it to the activities used in the reference method.

3.6.2.5 Enzymatic activity unit conversions:

1 HUT = 6.5 USP (Ianiro et al., 2016)
1 USP = 1 IU = 1 U (Russ Rowlett, 2018)

3.6.2.6 Enzyme activities per capsule:

Protease 3.0 = 25 SAPU (negligible)
Protease 4.5 = $40000\ \mathrm{HUT} * 6.5\ \mathrm{U} = 260000\ \mathrm{U}$
Protease 6.0 = $7500\ \mathrm{HUT} * 6.5\ \mathrm{U} = 48750\ \mathrm{U}$

3.6.2.7 Enzyme activity (U) per gram enzyme mix:

Average mass of enzyme mix per capsule: 0.341958 g
Combined protease activity per gram of enzyme supplement = $\frac{260000\ \mathrm{U} + 48750\ \mathrm{U}}{0.341958\ \mathrm{g}} = 902888.66\ \mathrm{U\ g^{-1}}$
Volume SGF: 11.5 mL
Volume SIF: 19 mL
Enzyme activity in SGF: $670\ \mathrm{U/mL} * 11.5\ \mathrm{mL} = 7705\ \mathrm{U}$
Enzyme activity in SIF: $16\ \mathrm{U/mL} * 19\ \mathrm{mL} = 304\ \mathrm{U}$
Mass of enzyme mix needed for 11.5 mL SGF: $\frac{7705\ \mathrm{U}}{902888.66\ \mathrm{U\ g^{-1}}} = 0.00853372\ \mathrm{g}$
Mass of enzyme mix needed for 19 mL SIF: $\frac{304\ \mathrm{U}}{902888.66\ \mathrm{U\ g^{-1}}} = 0.0000336697\ \mathrm{g}$

3.6.2.8 Gastric pH

Gastric pH was calculated using equation 4 which calculates the gastric acidification curve (Ménard *et al.*, 2018).

$$\mathrm{pH} = -0.015 * \mathrm{GE}_{1/2} + 6.52 \qquad (4)$$

$$\text{Gastric pH} = -0.015*(78*1.073865) + 6.52 \approx 5.26$$

Since the calculated gastric pH for 6- to 12-month-old children (5.26) was not much different from that of newborn children (5.3), it was decided to keep the original pH values throughout the method.

3.6.2.9 Determining the amount of HCl solution and NaOH solution for pH adjustment

The volume of 1 mol L^{-1} HCl-solution and 1 mol L^{-1} NaOH-solution needed to set the pH of the samples to 5.3, 7.0 and 6.6 was calculated by measuring the pH of a wet sample under the different conditions for each step using a pH-meter (Metrohm, model 744) and adding drops of HCl solution and NaOH solution using a plastic Pasteur pipette and converting the number of drops that resulted in the target pH to mL. Each drop was approximated to 0.05 mL. The respective volumes to reach the target pH in each step is presented as follows:

Sample + SGF pH ~4.6 ⟶ pH ~5.3 = 40 drops (2.0 mL) of 1 mol L^{-1} NaOH-solution
Sample + SGF pH ~5.3 ⟶ pH ~7 = 15 drops (0,75 mL) of 1 mol L^{-1} NaOH-solution
Sample + SGF + SIF pH ~7 ⟶ pH ~6.6 = 3 drops (0,15 mL) of 1 mol L^{-1} HCl-solution

3.6.2.10 Gastric and intestinal salt content

The salt content of the SGF and SIF solutions used in the reference method were used without modification and consisted of 5.49 mg mL^{-1} NaCl and 0.97 mg mL^{-1} KCl in the SGF solution, and 9.58 mg mL^{-1} NaCl, 0.75 mg mL^{-1} KCl, 7.14 mg mL^{-1} $NaHCO_3$ and 0.33 mg mL^{-1} $CaCl_2$ in the SIF solution. Due to unavailability of bile salts during the time frame of the project, these were disregarded.

3.6.3 Complete sequential *in vitro* digestion

3.6.3.1 Simulated gastric and intestinal fluid compositions

Using the modified parameters calculated from the reference method, the final simulated secretion fluid compositions can be seen in table 5. 1 liter of each solution was prepare in 1 liter PP flasks.

Table 5. Simulated secretion fluid compositions (per 9.5 g sample)

Component	Simulated gastric fluid	Simulated intestinal fluid
DI water	5.8 mL	9.5 mL
Enzyme supplement	4.3 mg	0.2 mg
NaCl	31.6 mg	91.0 mg
KCl	5.6 mg	7.1 mg
$NaHCO_3$	-	67.8 mg
$CaCl_2$	-	3.2 mg

3.6.3.2 *In vitro* pH and enzyme influence control

In addition to the complete *in vitro* digestion a series of *in vitro* control solutions were produced that excluded addition of acid and base from the procedure and enzyme supplement from the secretion fluid matrices. Three different types of control procedures were performed, "No acid" that did not receive pH adjustment during the extraction process, "No enzyme" that used SGF and SIF solutions that didn't contain any enzyme supplement, and "No acid or enzyme" that excluded both of the mentioned parameters. These control solutions were intended to result in data that could be used to determine the influence of pH and enzymes on the extractable mass content as well as the influence of pH on the enzymatic activity. Each control solution was made using sample 1 and prepared in six replicates each.

3.6.3.3 Procedural blanks

Procedural blanks were prepared for the full HNO_3 digestion, water leaching and *in vitro* digestion as well as for the "No acid", "No enzyme" and "No acid or enzyme" controls. Each blank was prepared in six replicates except for the HNO_3 and water leaching blanks that were singles.

3.6.3.4 Gastric phase aliquot

After the gastric phase extraction a 1.0 mL aliquot of all replicates of sample 1 and the pH and enzyme control solutions were taken using an auto-pipette to inspect the midway extraction progress.

3.6.4 Complete sequential *in vitro* digestion method

The following procedure refers to the *in vitro* and *in vitro* control methods. The *in vitro* controls deviate according to the previously mentioned *pH and enzyme influence control* setup.

9.50 g of sample 1 weighed to the nearest 0.1 mg was transferred to 50 mL PP-tubes and added with 5.8 mL of SGF solution each and the pH was adjusted to ~5.3 with 2.0 mL of 1 mol L^{-1} NaOH using an auto-pipette. All samples were then placed in a shaking water bath at 37°C for 60 min. 0.75 mL of 1 mol L^{-1} NaOH solution was added to each sample to adjust the pH to ~7. At this point a 1.0 mL gastric phase aliquot from the solution containing sample 1 and all control solutions were taken and set aside. 9.5 mL of SIF solution was added to the sample + SGF solutions. The solutions were set to pH 6.6 using 0.15 mL of 1 mol L^{-1} HCl-solution and placed back in the shaking water bath for another 60 min at 37°C. After incubation the solutions were centrifuged at 6000 RCF for 10 minutes resulting in a clear supernatant with only minor amounts of noticeable suspended matter. The supernatant was filtered through a 0.2 µm syringe filter and diluted by a factor of 50 using DI water as well as treated with 50 µL of concentrated

HNO_3-solution. 100 µL of Rh IS was added and the solutions were analyzed using ICP-MS. The control solutions were complemented with a MP-AES analysis. An overview of the *in vitro* digestion method can be seen in figure 5. The gastric phase aliquots were completed by centrifuging and filtration the same way as the fully digested samples.

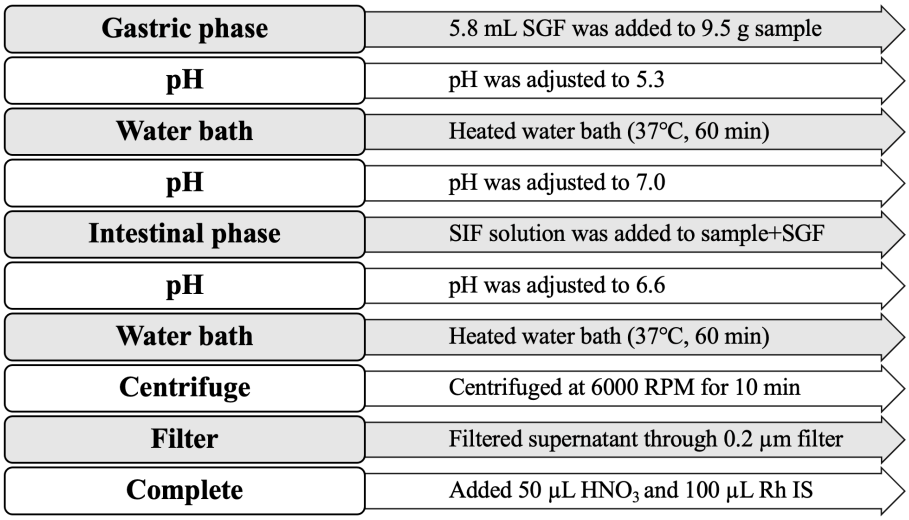

Figure 5. Progression chart overview of sequential *in vitro* digestion

3.7 ICP-MS model and settings

Table 6. ICP-MS model and settings

Model	Agilent 7500cX (Agilent, Japan)
Output	1500 W
Argon flows	Coolant: 15 L min^{-1} Auxiliary: 0.9 L min^{-1} Nebulizer: 0.2 L min^{-1}
Sample flow	0.3 mL min^{-1}
Nebulizer	MicroMist
Spray chamber	Scott double pass

Isotopes: ^{7}Li, ^{51}V, ^{59}Co, ^{60}Ni, ^{75}As, ^{82}Se, ^{111}Cd and ^{208}Pb (where ^{208}Pb is a combination of isotopes ^{204}Pb, ^{206}Pb, ^{207}Pb and ^{208}Pb).
Collision mode was used for isotopes ^{51}V, ^{75}As, ^{82}Se to minimize di- and poly-atomic interferences.

3.8 MP-AES model and settings

Table 7. MP-AES model and settings

Setting	Value
Number of replicates	3
Pump speed	15 RPM
Uptake time	88 s
Fast pump	yes
Rinse time	30 s
Fast pump	yes
Stabilization time	15 s
Number of pixels	3
correlation coefficient limit	0.9990
Number of standards	5 (0.5, 1, 3, 5 and 10 mg L^{-1})

Analytes: Li (670.784 nm), Ni (352.454 nm) and V (438.472 nm)

3.9 Statistical analysis

Since bio-accumulation of trace elements in plants and animals as well as the chemical reactions that were relevant for the methods are natural phenomena the data was assumed to have a gaussian distribution (Brereton, 2014). For all sample and blank replicates the mean and standard deviations based on n-1 were calculated using Microsoft Excel (version 16.57). Relative standard deviation (RSD) was calculated using formula (5).

$$\text{RSD}\ (\%) = \frac{s}{\bar{x}} * 100 \qquad (5)$$

Outliers were determined from blank corrected data using a two-step procedure. The first step was by using the 1.5xIQR rule to highlight potential outliers. The 1.5xIQR (1.5 x Inner Quartile Range) rule is used by calculating the inner quartile range of a set of values and multiplying it by 1.5 in both directions. If a data point value is outside this extended range it is considered an outlier. The second step was plotting the data and visually confirming if the calculated outliers from the 1.5xIQR test were visually different from the rest of the values. If both tests were positive then the data point/replicate was omitted when calculating the mean and standard deviations. Methodological LOD and LOQ could not be calculated since the methodological blanks had values below the instrumental LOQ. The instrumental LOQ was used to calculate a Least Quantifiable Mass Content (LQMC) level for each analyte in every matrix using formula 6.

$$\text{Least quantifiable mass content } \omega\ (\mu g\ g^{-1}) = \frac{\text{instrumental LOQ } \gamma\ [\mu g\ L^{-1}] * \text{sample volume (L)} * \text{dilution volume (L)}}{\text{mean sample mass (g)}} \qquad (6)$$

Individual t-tests were performed between the full *in vitro* and full HNO_3 digestion methods using all replicates from all six samples.

4. RESULTS AND DISCUSSION

4.1 Method validation

4.1.1 ICP-MS calibration standard ranges

ICP-MS calibrations standard ranges and R^2 values for each element are summarized in table 8.

Table 8. Element specific ICP-MS calibration concentration ranges and respective R^2 values. Using ICP multi element standard solution VI from Merck. Date: 220309

	^{7}Li	^{51}V	^{50}Co	^{60}Ni	^{75}As	^{82}Se	^{111}Cd	^{208}Pb
Range γ (µg L^{-1})	0.01 - 1	0.001 - 1	0.001 - 1	0.01 - 100	0.01 - 10	0.01 - 10	0.001 - 1	0.001 - 1
R^2	0.991359	0.999998	0.9999998	0.999998	0.99998	0.99990	0.99994	0.999831

Only one set of calibration data from the first analysis occasion (date: 220309) was supplied by the ICP-MS operator. Preferably individual calibration results for each analysis case should be presented. Complete calibration data from 220309 is listed in table 1 in the appendix and calibration curves are plotted in figures 1-8 in the appendix.

4.1.2 Least quantifiable mass content

The calculated LQMC in µg g^{-1} for each digestion method can be seen in tables 9 and 10. Selenium was under the instrumental LOQ for all digestion methods and is therefore omitted from most subsequent tables and graphs.

Table 9. ICP-MS Least quantifiable mass content ω (µg g^{-1}) in HNO_3 digested samples. Mean dry mass of samples: 0.20 g (± 0.001 SD).

	^{7}Li	^{51}V	^{50}Co	^{60}Ni	^{75}As	^{82}Se	^{111}Cd	^{208}Pb
Least quantifiable mass content ω (µg g^{-1})	0.00313	0.00313	0.000140	0.0313	0.00625	0.494	0.00313	0.00313

Table 10. ICP-MS Least quantifiable mass content ω (µg g^{-1}) in artificial *in vitro* digested samples.

Least quantifiable mass content ω (µg g^{-1})	Mean dry mass (g)	^{7}Li	^{51}V	^{50}Co	^{60}Ni	^{75}As	^{82}Se	^{111}Cd	^{208}Pb
Full *in vitro* procedure	1.23	0.00655	0.00655	0.00327	0.00655	0.00655	0.877	0.00327	0.00327
No acid	1.22	0.00743	0.00743	0.00372	0.00743	0.00743	0.996	0.00372	0.00372
No enzyme	1.23	0.00742	0.00742	0.00371	0.00742	0.00742	0.994	0.00371	0.00371
No acid or enzyme	1.22	0.00743	0.00743	0.00371	0.00743	0.00743	0.996	0.00371	0.00371

The LQMC value of cobalt in HNO_3 solution (see table 9) is questionably low and should be regarded with some skepticism.

4.1.3 Statistical comparison

t-tests between the *in vitro* and HNO_3 digestion methods showed a statistical difference between the two methods for all analytes except lithium. Li ($p = 0.7$), V ($p = 2.29*10^{-18}$), Co ($p = 4.81*10^{-17}$), Ni ($p = 1.18*10^{-6}$), As ($p = 0.0492$), Cd ($p = 1.03*10^{-17}$) and Pb ($p = 1.78*10^{-5}$).

t-test between the three control procedures and the full *in vitro* digestion indicated sporadic significant differences except for cadmium and cobalt that exhibited significant differences between the full *in vitro* digestion and all the control procedures. statistical significance for lead could not be determined since no lead was detected in full *in vitro* sample 1. The respective p-values are listed in table 11.

Table 11. t-test p-values of extracted mass content between full *in vitro* digestion samples and control samples without pH adjustment (no acid), "enzyme" and "pH adjustment and enzyme" respectively. Gray tinted cells highlights p-values <0.05.

Methods	^{7}Li	^{51}V	^{59}Co	^{60}Ni	^{75}As	^{82}Cd	^{208}Pb
In vitro / no acid	$9.30*10^{-3}$	0.289	$0.401*10^{-3}$	0.0957	0.356	0.0156	-
In vitro / no enzyme	0.0885	0.0116	$8.15*10^{-3}$	0.334	0.0679	0.0134	-
In vitro / no acid or enzyme	0.604	0.532	$6.60*10^{-6}$	0.0107	0.210	$1.12*10^{-3}$	-

4.2 Element specific results

4.2.1 Mass contents overview

Table 12. ICP-MS data. Calculated mean dry mass content of Li, V, Co and Ni in HNO_3 digestion and water leaching samples.

Sample ID	^{7}Li ω (µg g^{-1})		^{51}V ω (µg g^{-1})		^{59}Co ω (µg g^{-1})		^{60}Ni ω (µg g^{-1})	
	mean	SD	mean	SD	mean	SD	mean	SD
Sample 1	0.0436	0.0155	0.00915	0.00191	0.0243	0.00117	0.409	0.0822
Sample 2	0.0474	0.0124	0.0288	0.00248	0.0269	0.000457	0.833	0.274
Sample 3	0.0387	0.0154	0.0132	0.00442	0.0281	0.00233	1.21	0.896
Sample 4	0.111	0.0250	0.00974	0.00407	0.0139	0.000307	0.442	0.0337
Sample 5	0.0642	0.0202	0.0187	0.00263	0.0527	0.00160	0.566	0.0895
Sample 6	0.0331	0.0108	0.0241	0.00305	0.0274	0.00250	0.666	0.738
Sample 1 (water leaching)	0.0325	0.0169	0.00258	0.00148	0.0165	0.00171	0.133	0.0306
Enzyme supplement	0.0132	0.00851	0.693	0.0273	0.0934	0.00534	1.23	0.0141

Table 13. ICP-MS data. Calculated mean dry mass content of As, Cd and Pb in HNO_3 digestion and water leaching samples.

Sample ID	^{75}As ω (µg g^{-1})		^{111}Cd ω (µg g^{-1})		^{208}Pb ω (µg g^{-1})	
	mean	SD	mean	SD	mean	SD
Sample 1	0.0169	0.0122	0.0341	0.00391	0.0644	0.0287
Sample 2	0.0435	0.00689	0.0260	0.000659	0.0905	0.0562
Sample 3	0.0119	0.00346	0.0614	0.00359	0.410	0.163
Sample 4	0.00492	0.00124	0.0397	0.00477	0.0359	0.0111
Sample 5	0.0188	0.00881	0.0343	0.000748	0.0576	0.00659
Sample 6	0.0132	0.00853	0.0401	0.00260	0.128	0.0147
Sample 1 (water leaching)	0.0421	0.0205	0.0234	0.00268	0.00791	0.00585
Enzyme supplement	0.365	0.0309	0.0180	0.00111	0.0276	0.00445

Table 14. ICP-MS data. Calculated mean dry mass content of Li, V, Co and Ni in full *in vitro* digestion samples.

Sample ID	^{7}Li ω (µg g^{-1})		^{51}V ω (µg g^{-1})		^{59}Co ω (µg g^{-1})		^{60}Ni ω (µg g^{-1})	
	mean	SD	mean	SD	mean	SD	mean	SD
Sample 1	0.0548	0.00713	0.00130	0.0019	0.0125	0.000216	0.0995	0.0174
Sample 2	0.0518	0.00749	0.0116	0.0021	0.0128	0.000674	0.131	0.0180
Sample 3	0.0445	0.00657	<0.00655		0.0143	0.000327	0.0793	0.0201
Sample 4	0.109	0.00396	0.00187	0.0022	0.00686	0.000365	0.163	0.0224
Sample 5	0.0589	0.00700	0.00330	0.0014	0.0292	0.00101	0.174	0.0219
Sample 6	0.0401	0.00396	0.0119	0.0029	0.0159	0.000578	0.103	0.0249

Table 15. ICP-MS data. Calculated mean dry mass content of As, Cd and Pb in full *in vitro* digestion samples.

Sample ID	^{75}As ω (µg g^{-1})		^{111}Cd ω (µg g^{-1})		^{208}Pb ω (µg g^{-1})	
	mean	SD	mean	SD	mean	SD
Sample 1	0.00434	0.00292	0.00374	0.000981	<0.00327	
Sample 2	0.0248	0.00776	0.00164	0.000590	0.00615	0.00487
Sample 3	0.00108	0.00890	0.00539	0.00113	0.000376	
Sample 4	0.00353	0.00197	0.00783	0.00132	0.00368	
Sample 5	0.00331	0.00160	0.00769	0.00144	<0.00327	
Sample 6	0.0290	0.0115	0.00858	0.00165	0.0193	0.00260

Table 16. ICP-MS data. Calculated mean dry mass content of Li, V, Co and Ni in *in vitro* control procedure samples containing sample 1.

Procedure	^{7}Li ω (µg g^{-1})		^{51}V ω (µg g^{-1})		^{59}Co ω (µg g^{-1})		^{60}Ni ω (µg g^{-1})	
	mean	SD	mean	SD	mean	SD	mean	SD
Full *in vitro* digestion	0.0548	0.00713	0.00130	0.00132	0.0125	0.000216	0.0995	0.0174
No acid	0.0375	0.00456	<0.00743		0.00845	0.000322	0.184	0.0956
No enzyme	0.0629	0.0124	0.00486	0.00232	0.00974	0.00116	0.114	0.0312
No acid or enzyme	0.0518	0.00660	0.000490	0.000490	0.00504	0.000129	0.148	0.0227

Table 17. ICP-MS data. Calculated mean dry mass content of As, Cd and Pb in *in vitro* control procedure samples containing sample 1.

Procedure	$^{75}As\ \omega\ (\mu g\ g^{-1})$		$^{111}Cd\ \omega\ (\mu g\ g^{-1})$		$^{208}Pb\ \omega\ (\mu g\ g^{-1})$	
	mean	SD	mean	SD	mean	SD
Full *in vitro* digestion	0.00439	0.00292	0.00374	0.000981	<0.00327	
No acid	0.00737	0.00466	0.00148	0.000665	0.00126	0.000687
No enzyme	0.00904	0.00186	0.00198	0.00119	0.0242	0.00368
No acid or enzyme	0.00984	0.00583	0.000491	0.000391	0.00845	0.00460

4.2.2 HNO_3 digestion concentration test results

The extracted mass contents for the test of different concentrations of HNO_3 digestion solutions can be seen in figure 6 to 9. Digestion by 20% (~2.8 mol L^{-1}) HNO_3 solution resulted in RSD values between 0.7% and 142% (n = 3), 60% (~8.4 mol L^{-1}) HNO_3 solution in RSD values between 1.5% and 16% (n = 3) and 100% (~14 mol L^{-1}) HNO_3 solution in RSD values between 2.1% and 82% (n = 3). The results suggested that digestion using the 60% HNO_3 solution gave the highest and most stable signal for the highest number of analytes of interest compared to the 20% and 100% HNO_3 solutions. The mass content recoveries for each concentration were not consistent between elements and it is important to notice that none of the solutions resulted in the highest mass content or lowest SD for all of the analytes. Based on this a compromise was made to use a 60% HNO_3 solution for the complete acid digestion.

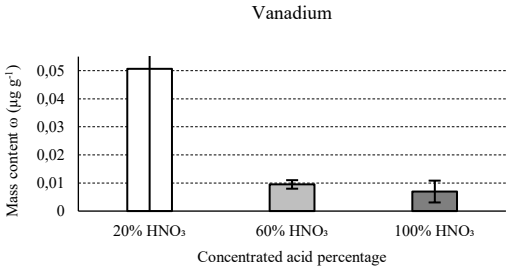

Figure 6. Dry mass content of vanadium in Sample 1. Extracted using three different concentrations of HNO_3 and analyzed using ICP-MS. Error bars represent ± standard deviation.

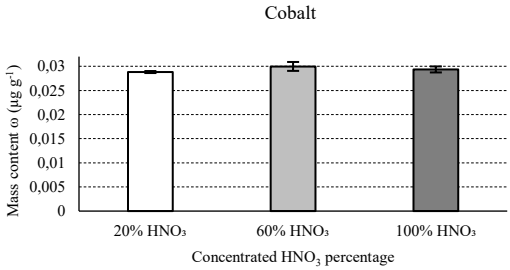

Figure 7. Dry mass content of cobalt in Sample 1. Extracted using three different concentrations of HNO_3 and analyzed using ICP-MS. Error bars represent ± standard deviation.

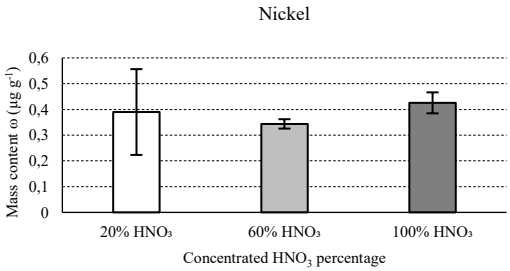

Figure 8. Dry mass content of nickel in Sample 1. Extracted using three different concentrations of HNO_3 and analyzed using ICP-MS. Error bars represent ± standard deviation.

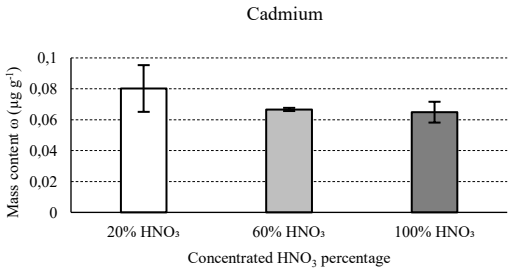

Figure 9. Dry mass content of cadmium in Sample 1. Extracted using three different concentrations of HNO_3 and analyzed using ICP-MS. Error bars represent ± standard deviation.

4.2.3 Lithium

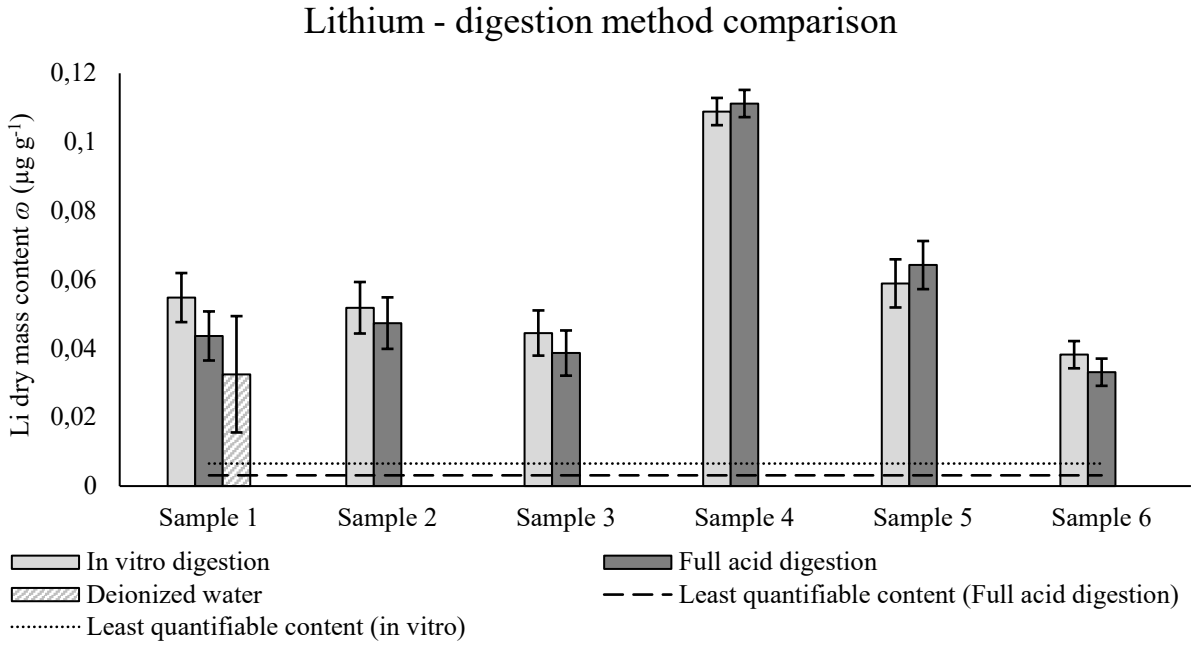

Figure 10. ICP-MS data. Comparison of measured mass content of lithium between full HNO_3 digested (dark gray), *in vitro* digested (light gray) and DI water leached (striped) samples. The dotted line represents the least quantifiable mass content limit of *in vitro* procedure. The dashed line represents least quantifiable content limit of HNO_3 procedure. Error bars signify ± standard deviation.

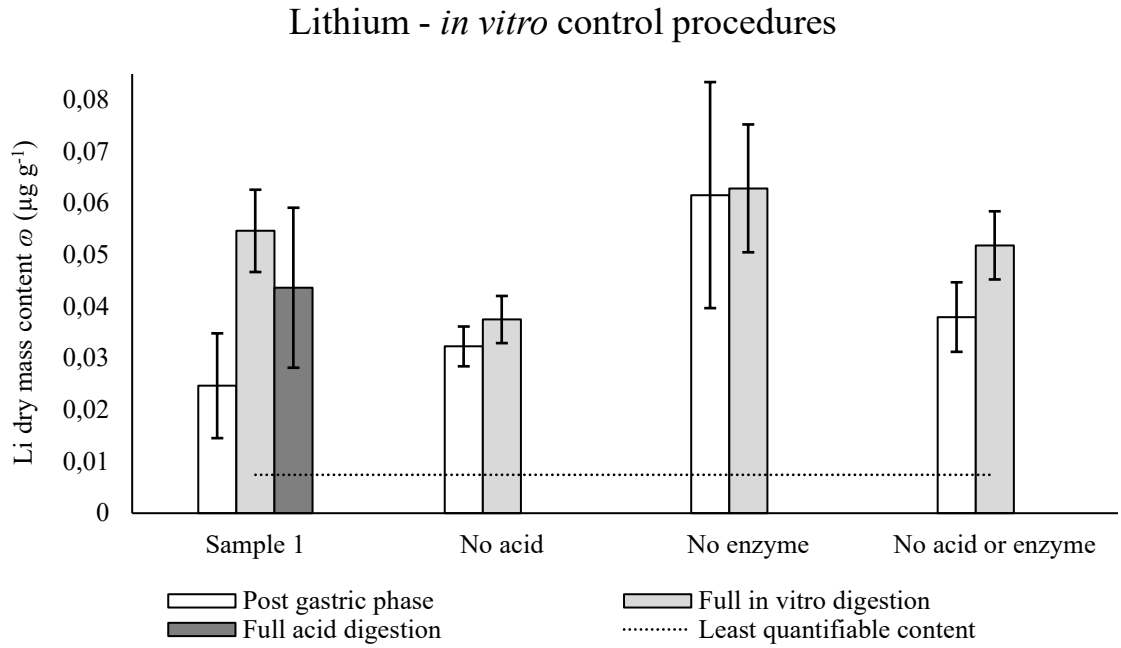

Figure 11. ICP-MS data. Comparison of measured mass content of lithium between full HNO_3 digested (dark gray), sequential *in vitro* digested (light gray) and post gastric phase *in vitro* aliquot (white) samples. The dotted line represents the least quantifiable mass content limit of *in vitro* procedure. Error bars signify ± standard deviation.

The mean values for lithium content showed no statistical difference between any of the digestion methods for any of the samples (figure 10). This could be a result of Li^+ readily dissociating into the aqueous phase of the solutions similarly to other group 1 elements such as Na^+. The highest recovery was found in sample 4. Sample 4 does not contain the highest amount of any ingredient or nutritional content making it difficult to elucidate the almost twice as high content. Possible explanations for this could be a high lithium concentration in the soil used to grow the wheat for the pasta or contamination during the production process.

4.2.4 Vanadium

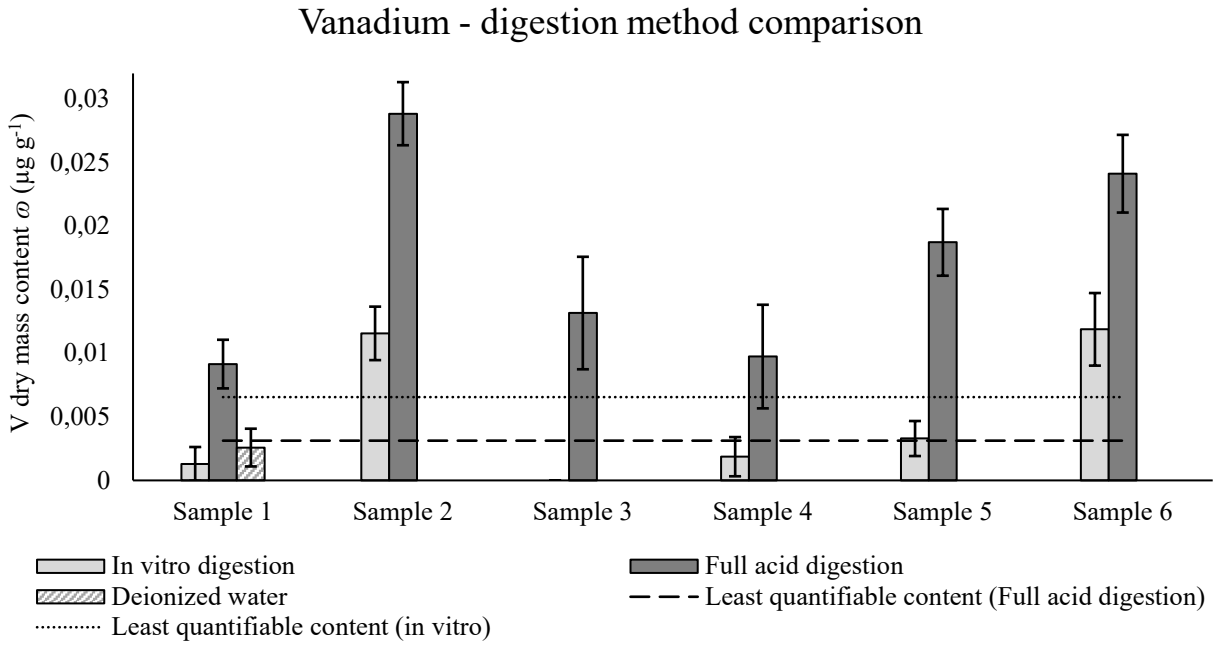

Figure 12. ICP-MS data. Comparison of measured mass content of vanadium between full HNO_3 digested (dark gray), *in vitro* digested (light gray) and DI water leached (striped) samples. The dotted line represents the least quantifiable mass content limit of *in vitro* solutions. The dashed line represents least quantifiable content limit of HNO_3 solutions. Error bars signify ± standard deviation.

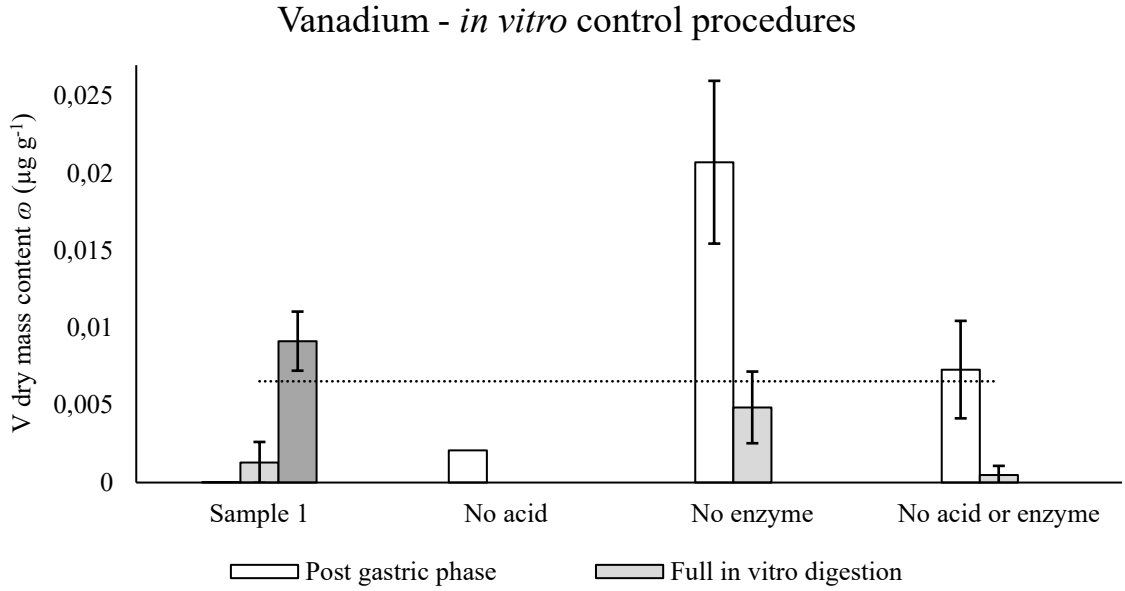

Figure 13. ICP-MS data. Comparison of measured dry mass content of vanadium between full HNO_3 digested (dark gray), sequential *in vitro* digested (light gray) and post gastric phase *in vitro* aliquot (white) samples. The dotted line represents the least quantifiable mass content limit of *in vitro* procedure. Error bars signify ± standard deviation.

The ICP-MS results of vanadium had mass content RSD values ranging between 19% and 102% in the *in vitro* digested samples and 8.6% and 42% for HNO_3 digestion. All HNO_3 digested samples had mass content with SD ranges over the LQMC while *in vitro* digested samples 1, 4 and 5 were below the LQMC and sample 3 was under the instrumental LOQ (table 14). Even though the three control procedures for vanadium did not produce any evidence of protein binding affinity (figure 13) with the full *in vitro* controls having mass content recoveries under the LQMC, the HNO_3 digestion mass content recoveries of samples 1-5 (figure 12) follow a similar pattern to their specified protein contents (table 2) of 2.3 g/100 g, 3.4 g/100 g, 2.8 g/100 g, 3.1 g/100 g and 3.5 g/100 g respectively supporting the known protein binding properties of vanadium (Crans *et al.*, 2004). The reported level of daily intake to have an adverse effect, ~20000 µg/day (EFSA, 2006), is five orders of magnitude higher than the average mass content in the samples and therefore not near toxic levels.

4.2.5 Nickel

Results of nickel mass content in the HNO_3 digested samples (figure 14) were incohesive and had RSD values that ranged between 7.6% in sample 4 to 111% in sample 6. The *in vitro* digested samples had more stable mass content RSD values ranging between 12.6% and 25.4%. All samples had recoveries over the LQMC for all matrices. The only control procedures that showed a statistical difference was between full *in vitro* digestion and the control procedure without pH adjustment or enzymes (figure 15). Notice that the difference is that the control procedure had a higher mass recovery than the full *in vitro* digestion which is unlikely to be true. Samples 2, 4 and 5 had the highest *in vitro* digestion mass recoveries which corresponds well to the specified protein content (table 2) of those samples, indicating them being protein bound. The amounts of nickel found in the samples are not enough to come close to the dose of 1250 µg/day/kg BW that have shown adverse effects in rats (EFSA, 2006).

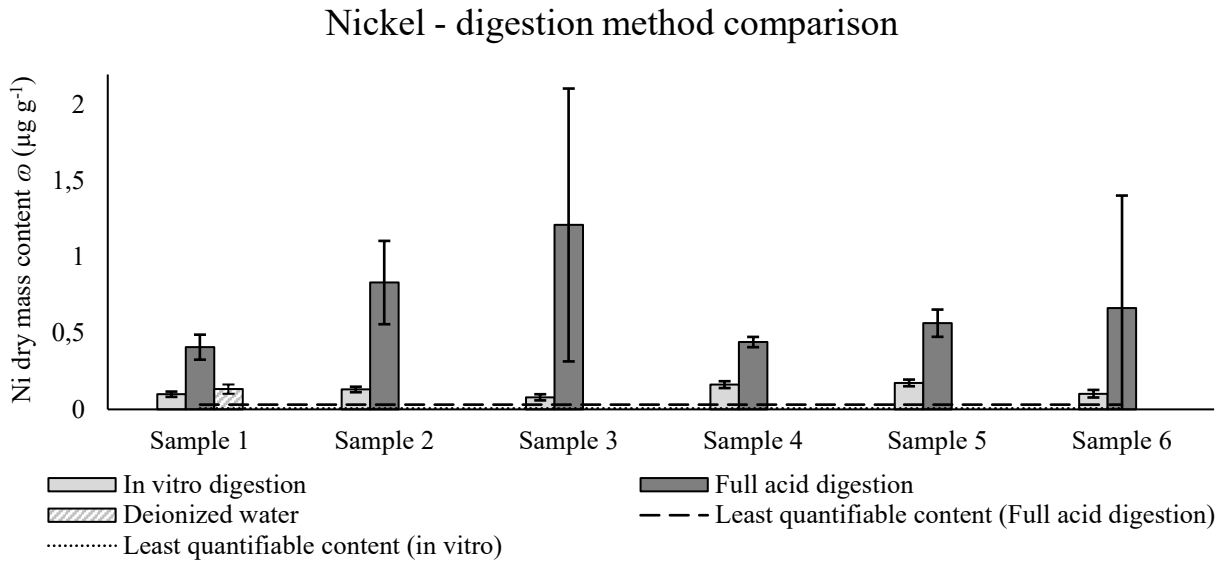

Figure 14. ICP-MS data. Comparison of measured mass content of nickel between in full HNO_3 digested (dark gray), *in vitro* digested (light gray) and DI water leached (striped) samples. The dotted line represents the least quantifiable mass content limit of *in vitro* procedure. The dashed line represents least quantifiable content limit of HNO_3 procedure. Error bars signify ± standard deviation.

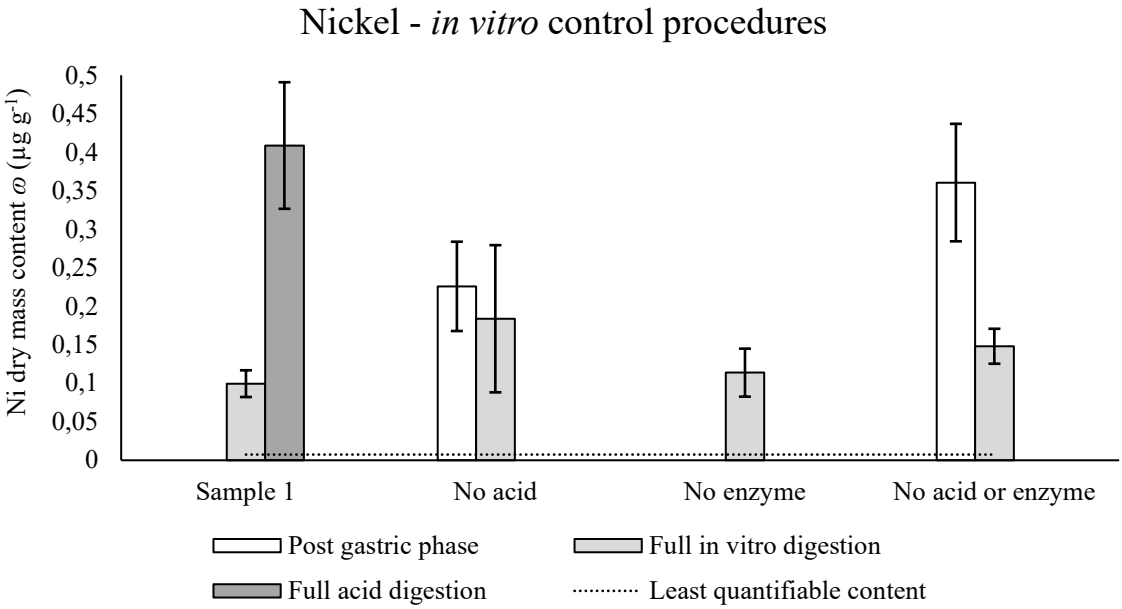

Figure 15. ICP-MS data. Comparison of measured mass content of nickel between full HNO_3 digested (dark gray), sequential *in vitro* digested (light gray) and post gastric phase *in vitro* aliquot (white) samples. The dotted line represents the least quantifiable mass content limit of *in vitro* procedure. represents the least quantifiable mass content limit of *in vitro* procedure. Error bars signify ± standard deviation.

4.2.6 Cobalt

The mass recoveries of cobalt (figure 16) had RSDs for all samples in all digestion methods ranging between 1.7% to 5.3% in the *in vitro* digested samples and 1.7% to 9.1% in the HNO_3 digestions. Water leaching of cobalt in sample 1 had an RSD of 10.4% which is slightly higher than the rest. All samples in all digestion matrices were well above their LQMC levels and t-test showed a significant difference between the full *in vitro* sample and all control procedures (table 11). The control procedure results (figure 17) indicate that cobalt is protein bound and that the proteases in the *in vitro* solutions are most active in a matrix adjusted to gastro-intestinal pH level. The high mass content in sample 5 could stem from its high protein content (table 2) but it does not explain why it is so much higher than sample 2 that has a similar protein content. It does have a ~55% higher pasta content giving it a higher percent of plant based proteins which could potentially be the cause since cobalt is shown to accumulate in wheat (Ejaz *et al.*, 2022). No specific data on harmful levels of cobalt were found in literature during the span of the project, but the average total content of 0.0323 µg per ~27 g of wet sample only makes up approximately 0.5% of the normal daily dietary intake of an adult human (EFSA, 2006).

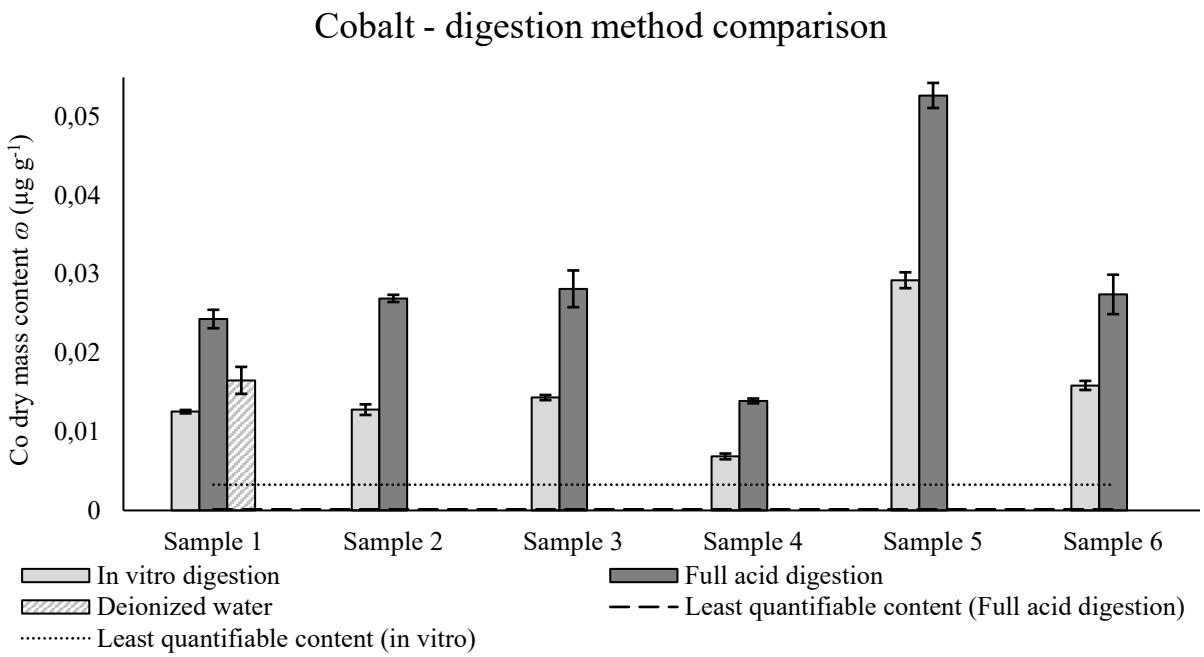

Figure 16. ICP-MS data. Comparison of measured dry mass content of cobalt between full HNO_3 digested (dark gray), sequential *in vitro* digested (light gray) and post gastric phase *in vitro* aliquot (white) samples. The dotted line represents the least quantifiable mass content limit of *in vitro* procedure. The dashed line represents the least quantifiable mass content limit of HNO_3 procedure. Error bars signify ± standard deviation.

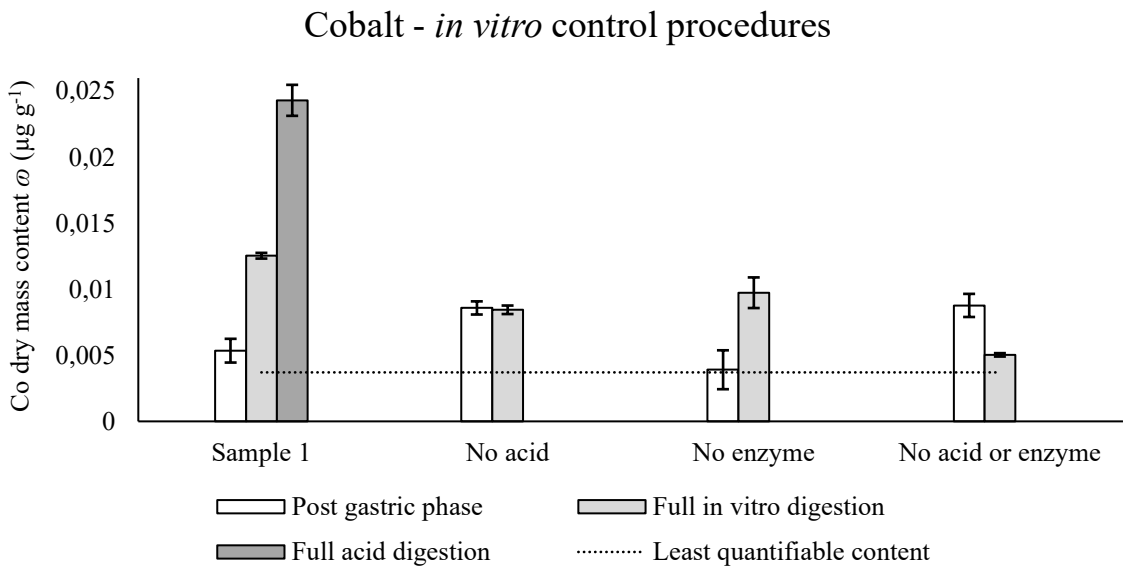

Figure 17. ICP-MS data. Comparison of measured dry mass content of cobalt between full HNO_3 digested (dark gray), sequential *in vitro* digested (light gray) and post gastric phase *in vitro* aliquot (white) samples. The dotted line represents the least quantifiable mass content limit of *in vitro* procedure. Error bars signify ± standard deviation.

4.2.7 Arsenic

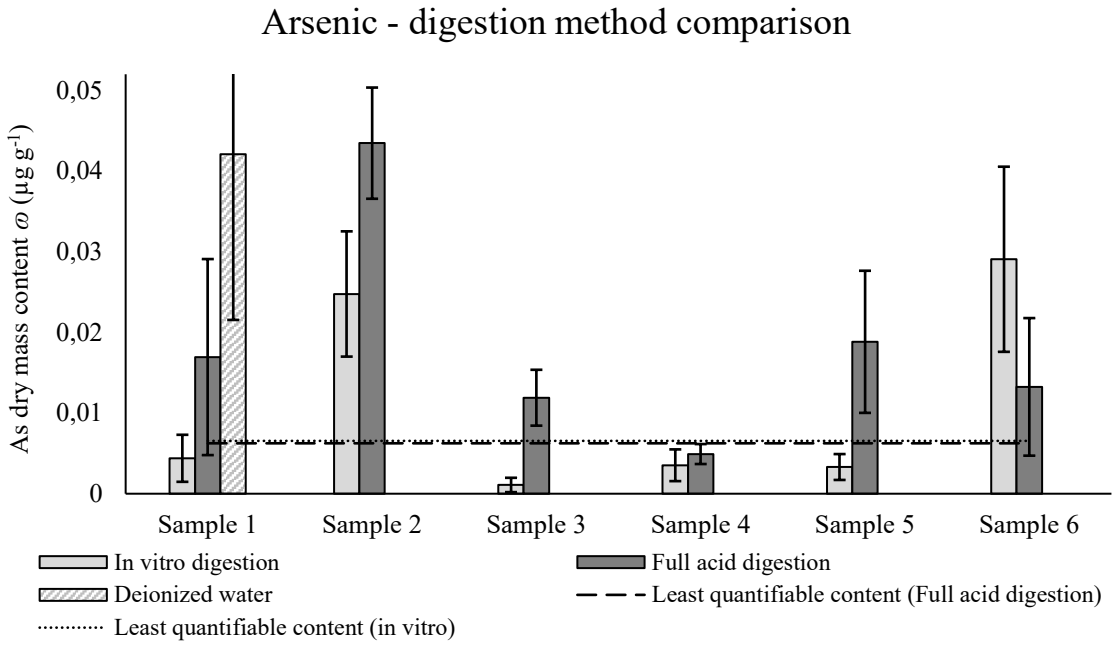

(EC) 1881/2006 As limit ω (µg g^{-1})	0.777	0.604	0.652	0.603	0.646	0.635

Figure 18. ICP-MS data. Comparison of measured mass content of arsenic between full HNO_3 digested (dark gray), *in vitro* digested (light gray) and DI water leached (striped) samples. The dotted line represents the least quantifiable mass content limit of *in vitro* procedure. The dashed line represents least quantifiable content limit of HNO_3 procedure. The table under the chart contains As ω (µg g^{-1}) maximum limit in baby food by (EC) 1881/2006. Error bars signify ± standard deviation.

In vitro and HNO_3 digestion results for arsenic (figure 18) as well as control procedures (figure 19) resulted in mass contents with high RSDs and content levels under or close to the LQMC and were therefore highly unreliable. None of the control procedures showed any statistical difference. The highest detected mass content was one order of magnitude lower than the maximum limit regulated by EU (*(EC) No 1881/2006*, 2006). None of the samples had content equal to or higher than the regulated maximum limit in baby food (*(EC) No 1881/2006*, 2006).

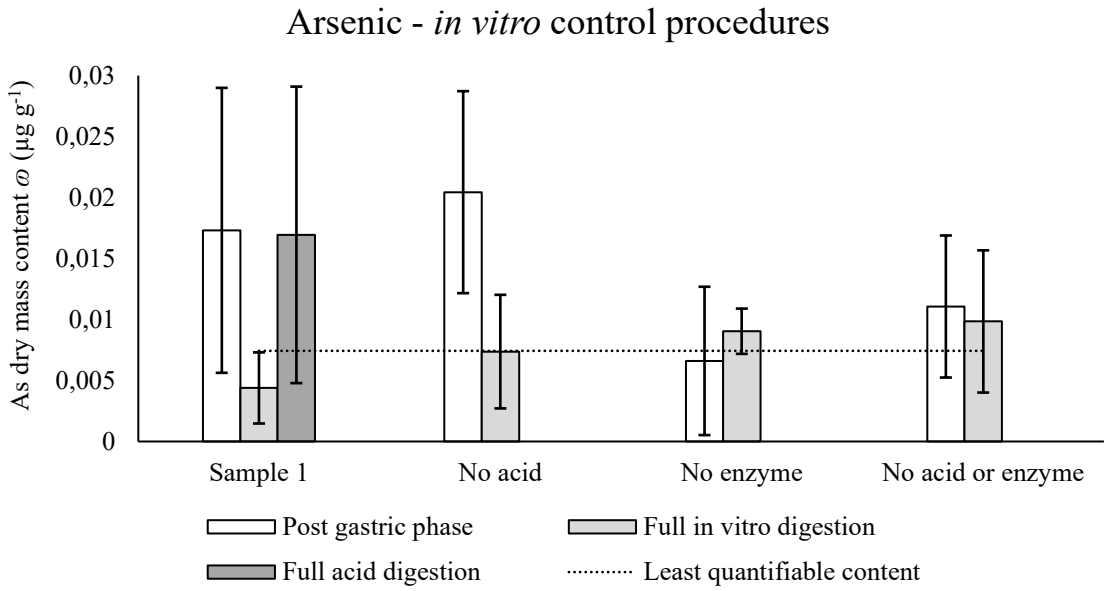

Figure 19. ICP-MS data. Comparison of measured mass content of arsenic between full HNO_3 digested (dark gray), sequential *in vitro* digested (light gray) and post gastric phase *in vitro* aliquot (white) samples. The dotted line represents the least quantifiable mass content limit of *in vitro* procedure. Error bars signify ± standard deviation.

4.2.8 Cadmium

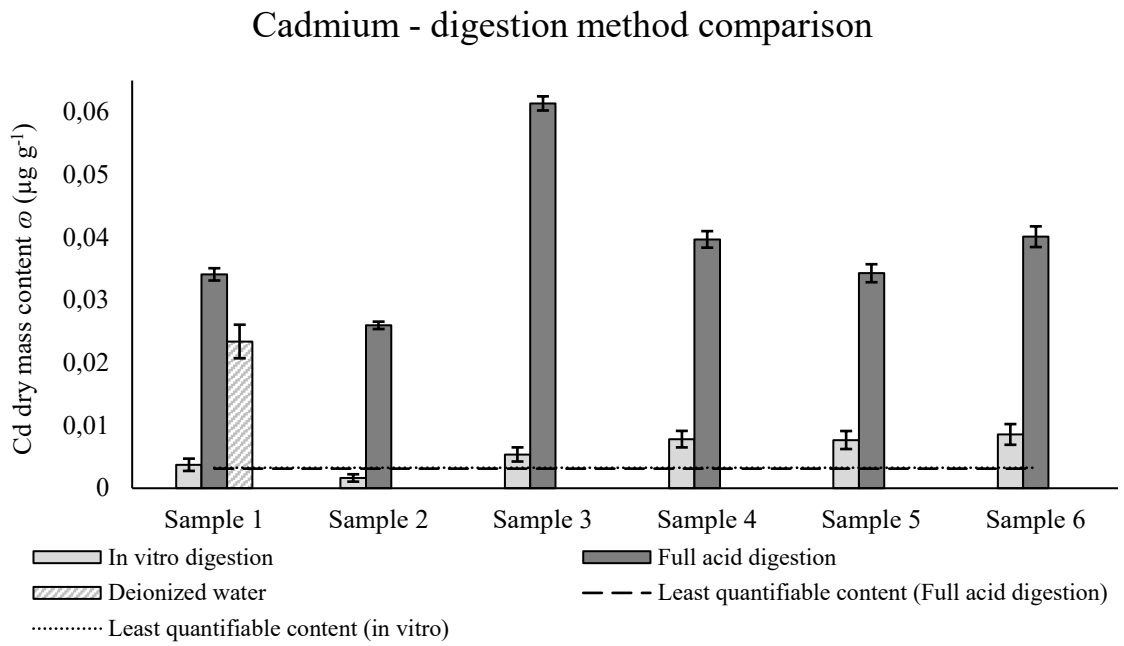

(EC) 1881/2006 Cd limit ϖ (µg g^{-1})	0.311	0.242	0.261	0.241	0.258	0.254

Figure 20. ICP-MS data. Comparison of measured mass content of cadmium between full HNO_3 digested (dark gray), *in vitro* digested (light gray) and DI water leached (striped) samples. The dotted line represents the least quantifiable mass content limit of *in vitro* procedure. The dashed line represents least quantifiable content limit of HNO_3 procedure. The table under the chart contains cadmium ϖ (µg g^{-1}) maximum limit in baby food by (EC) 1881/2006. Error bars signify ± standard deviation.

All full *in vitro* digested samples (figure 20) had cadmium contents close to the LQMC and for the control procedures (figure 21) they were all below the LQMC. Even though they could not be used at a quantitative level all control procedures displayed statistical difference against the full *in vitro* digestion and similarly to cobalt the matrix containing enzymes and had pH adjusted to gastro-intestinal levels showed a significantly higher mass content recovery, implying cadmium to be protein bound and extractable using the *in vitro* method. In the HNO_3 digestion method sample 3 the highest cadmium content at ~25% of the regulated maximum limit (*(EC) No 1881/2006*, 2006).

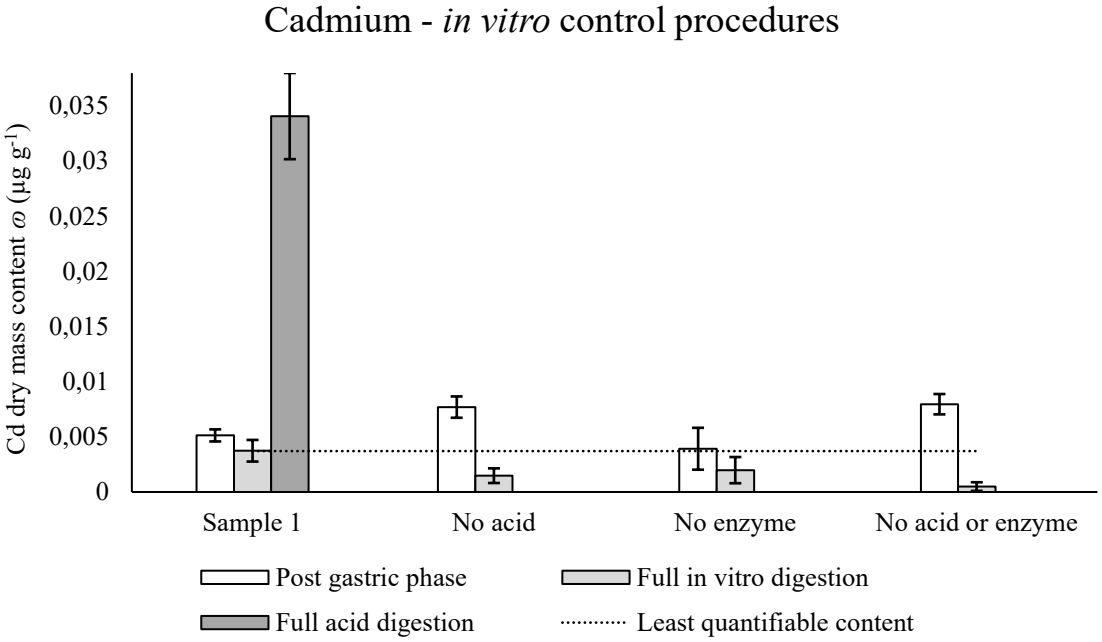

(EC) 1881/2006 Cd limit ϖ (µg g^{-1})	0.311	0.242	0.261	0.241	0.258	0.254

Figure 21. ICP-MS data. Comparison of measured mass content of cadmium between full HNO_3 digested (dark gray), full *in vitro* digested (light gray) and post gastric phase *in vitro* aliquot (white) samples. The dotted line represents the least quantifiable mass content limit of *in vitro* procedure. Error bars signify ± standard deviation.

4.2.9 Lead

Lead mass content in the control procedure digested samples without pH adjustment were both under the LQMC and the control procedure without enzymes was over the LQMC (figure 23). Only *in vitro* "no enzyme" is over. Lead was only quantifiable in sample 6 in the *in vitro* digested samples and at such low content that it was one order of magnitude lower than the EU limit (*(EC) No 1881/2006*, 2006). HNO_3 digestion results in a higher extraction vs *in vitro* and water (figure 22). No quantifiable lead content was over the maximum limit with statistical significance. A comparison with the measured lead mass content in wet baby food (wheat and rice based) by Livsmedelsverket in 2017 (Livsmedelsverket, 2018) were they found between 0.005 µg g^{-1} to 0.015 µg g^{-1} in 36 samples suggests that the highest HNO_3 extracted mass content of 0.00693 µg g^{-1} (sample 6 concerted to equivalent wet mass) in this project is at an expected level.

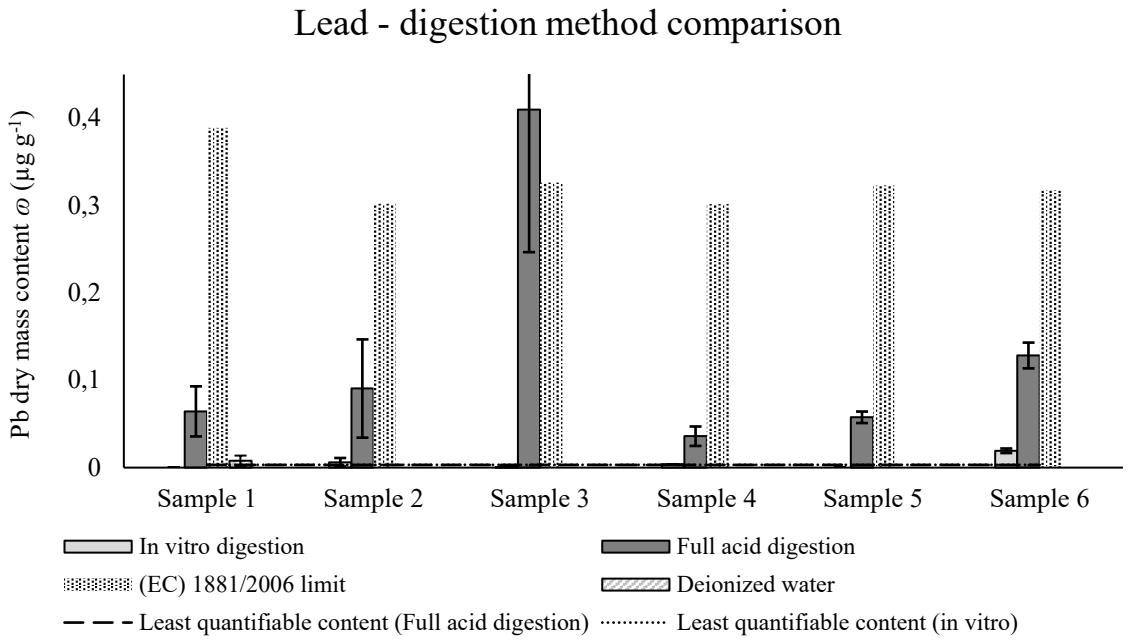

Figure 22. ICP-MS data. Comparison of measured mass content of lead between full HNO_3 digested (dark gray), *in vitro* digested (light gray) and DI water leached (striped) samples. The dotted line represents the least quantifiable mass content limit of *in vitro* procedure. The dashed line represents least quantifiable content limit of HNO_3 procedure. Lead ϖ (µg g^{-1}) maximum limit in dry baby food by (EC) 1881/2006. Error bars signify ± standard deviation.

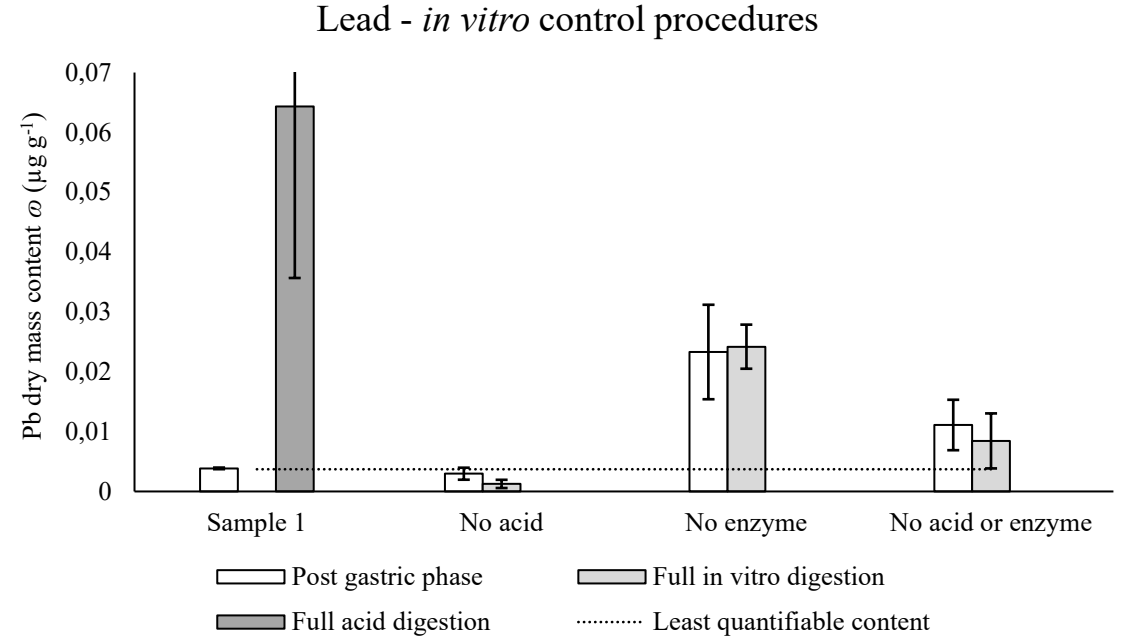

Figure 23. ICP-MS data. Comparison of measured mass content of lead between full HNO_3 digested (dark gray), sequential *in vitro* digested (light gray) and post gastric phase *in vitro* aliquot (white) samples. The dotted line represents the least quantifiable mass content by *in vitro* procedure. Error bars signify ± standard deviation.

4.3 MP-AES results

Table 18. MP-AES data. Mean concentration of Li, Ni and V in *in vitro* control procedures.

	Li 670.784 nm γ [µg L^{-1}]			Ni 352.454 nm γ [µg L^{-1}]			V 438.472 nm γ [µg L^{-1}]		
	mean	SD	95% CI	mean	SD	95% CI	mean	SD	95% CI
Full *in vitro* procedure	121	6.80	6.62	35.9	5.81	4.64	15.0	0.997	0.98
No acid	73.8	17.2	13.8	43.8	8.19	6.56	15.9	1.63	1.57
No enzyme	94.8	3.20	4.43	16.6	2.17	3.05	10.9	4.67	6.51
No acid or enzyme	59.0	14.0	11.2	26.3	2.24	2.16	12.3	5.09	4.08

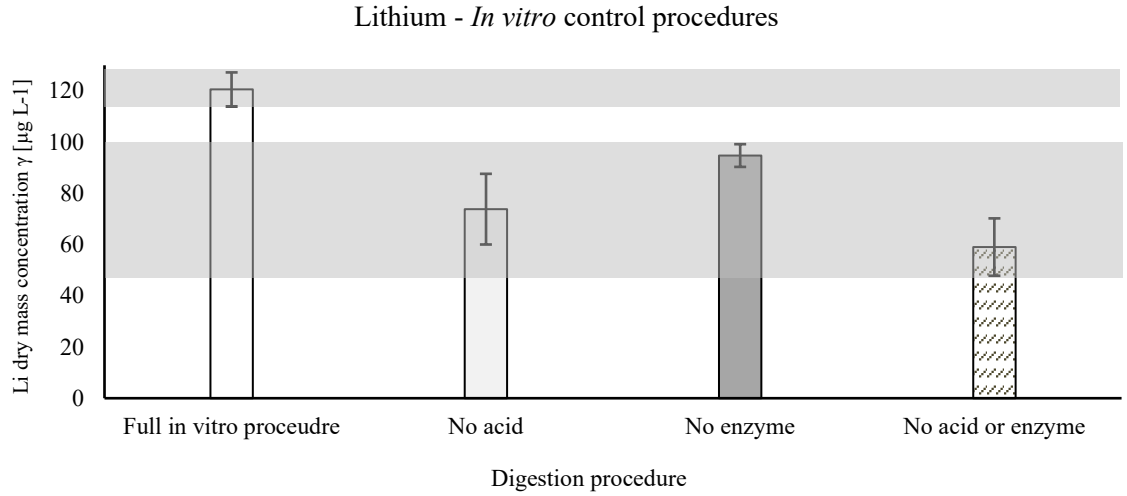

Figure 24. MP-AES data. Dry mass content comparison of lithium between full *in vitro* digestion and control procedures. Error bars represent 95% CI. The gray fields illustrates the full *in vitro* procedure 95% CI and combined 95% CI of the control procedures..

Due to the high Na^+ and Cl^- content of the matrices of the solutions obtained from the *in vitro* procedures the MP-AES results were not quantitatively reliable, but a comparison between the 95% confidence intervals for the different control procedures show that there is a difference between the full *in vitro* sample containing both enzyme supplement and undergoing pH adjustment. This supports the notion that similarly to cadmium and cobalt, lithium is protein bound and that the activity of the enzymes are pH dependent (figure 24). This relationship between the digestion procedures for lithium was not visible in the ICP-MS data (figure 11). Similar MP-AES data for nickel and vanadium (table 18) did not show any statistical significance between control procedures.

In summary the LQMC was generally high for all digestion procedures. Testing different concentrations of HNO_3 for full digestion of the samples indicated that ~8.4 mol L^{-1} HNO_3 solution resulted in the overall lowest RSDs and highest recoveries for the MTEs of interest. Selenium was not detectable in any sample by any method. Statistical comparison showed significant difference between all digestion methods and control procedures for cobalt and cadmium. A p-value of 0.7 in the comparison between the total content and *in vitro* recovery

for lithium showed that possibly all lithium is bio-accessible without any digestion needed. Vanadium, arsenic and lead had relatively high RSDs and LQMC levels and could not be quantified in all samples using the *in vitro* method. Nickel, cobalt and cadmium had recoveries above the LQMC in all samples using the HNO_3 digestion. Nickel and cobalt could be quantified in all samples via the *in vitro* method. The control procedure results indicated that the enzymes in the gastric and intestinal solutions were active and were pH dependent. Vanadium and cobalt seemed to have correlation between the quantified amount of analyte and the specified protein content of each sample which could be a sign of the elements protein binding properties. No sample contained toxic levels of any analyte except for sample 3 that had an average lead content above the maximum allowed amount as regulated by the Commission regulation (EC) 1881/2006, but a RSD that extended under it and thus cannot be determined to exceed the limit. The possibility of sample contamination also cannot be ruled out without further testing.

5. CONCLUSION

The element specific total content determined in HNO_3 digested samples are presented in table 19. The element specific content determined in artificial *in vitro* digested samples are presented in table 20. Outliers were omitted.

Table 19. ICP-MS data. Total extracted element specific mass content ω ($\mu g\ g^{-1}$) in HNO_3 digested baby food samples. Ranges represent replicates with lowest and highest quantified content.

Element	Sample 1	Sample 2	Sample 3	Sample 4	Sample 5	Sample 6
Lithium	0.0280 - 0.0645	0.0306 - 0.0622	0.0208 - 0.0564	0.08863 - 0.149	0.0446 - 0.0905	0.0169 - 0.0467
Vanadium	0.00815 - 0.0127	0.0274 - 0.0328	0.00874 - 0.0191	0.00518 - 0.0151	0.0157 - 0.0224	0.0215 - 0.0285
Cobalt	0.0257 - 0.0290	0.0295 - 0.0303	0.0288 - 0.0321	0.0166 - 0.0173	0.0536 - 0.0577	0.0276 - 0.0416
Nickel	0.309 - 0.539	0.483 - 1.20	0.586 - 2.45	0.408 - 0.488	0.472 - 0.706	0.317 - 1.98
Arsenic	0.00419 - 0.0308	0.0351 - 0.0538	0.00989 - 0.0171	0.00355 - 0.00596	0.00887 - 0.0313	0.00210 - 0.0242
Selenium	-	-	-	-	-	-
Cadmium	0.0298 - 0.0412	0.0259 - 0.0275	0.0586 - 0.0683	0.0332 - 0.0465	0.0343 - 0.0359	0.0386 - 0.0448
Lead	0.0381 - 0.112	0.0357 - 0.183	0.225 - 0.650	0.0211 - 0.0499	0.0508 - 0.0673	0.117 - 0.154

Table 20. ICP-MS data. Total extracted element specific mass content ω ($\mu g\ g^{-1}$) in artificial *in vitro* digested baby food samples. Ranges represent replicates with lowest and highest quantified content.

Element	Sample 1	Sample 2	Sample 3	Sample 4	Sample 5	Sample 6
Lithium	0.0428 -0.0631	0.0428 - 0.0626	0.0361 - 0.0539	0.105 - 0.115	0.0482 - 0.0691	0.0314 - 0.0409
Vanadium	0.000365 - 0.002239	0.00932 - 0.0152	-	$9.42*10^{-5}$ - 0.00386	0.00193 - 0.00509	0.00817 - 0.0157
Cobalt	0.0122 - 0.0127	0.0118 - 0.0138	0.0139 - 0.0147	0.00661 - 0.00749	0.0282 - 0.0309	0.0153 - 0.0165
Nickel	0.0752 - 0.127	0.100 - 0.146	0.0599 - 0.108	0.138 - 0.194	0.146 - 0.194	0.0793 - 0.139
Arsenic	0.00191 - 0.00757	0.0156 - 0.0356	0.000454 -0.00171	0.00154 - 0.00610	0.00173 - 0.00555	0.0155 - 0.0431
Selenium	-	-	-	-	-	-
Cadmium	0.00247 - 0.00479	0.000887 - 0.00245	0.00390 - 0.00655	0.00581 - 0.00922	0.00622 - 0.00953	0.00638 - 0.00985
Lead	-	0.00124 - 0.0124	-	-	-	0.0159 - 0.0232

- None of samples contained toxic levels of the MTEs of interest.

- The artificial *in vitro* method recovered 106% lithium, 35% vanadium, 53% cobalt, 18% nickel, 61% arsenic, 15% cadmium and 6% lead compared to the HNO_3 method which gives insight into the binding of the metals to the food matrix.

- The control procedure analyses for cadmium and cobalt using ICP-MS and lithium using MP-AES indicated that the enzymatic digestion was active as well as pH dependent.

- The obtained results show that the developed method is applicable as a simple and affordable alternative to more elaborate methods for screening or small scale analysis. Full establishment of the method requires further research and optimization of the method.

6. REFERENCES

Achour, L., Méance, S. and Briend, A. (2001) 'Comparison of gastric emptying of a solid and a liquid nutritional rehabilitation food', *European Journal of Clinical Nutrition*, 55(9), pp. 769–772. doi:10.1038/sj.ejcn.1601221.

Baird, C. and Cann, M.C. (2012) *Environmental chemistry*. 5th edition. New York: W.H. Freeman.

Bansal, S. and Asthana, S. (2018) 'Biologically Essential and Non-Essential Elements Causing Toxicity in Environment', *Journal of Environmental & Analytical Toxicology*, 08, pp. 3–4. doi:10.4172/2161-0525.1000557.

Bjørklund, G. *et al.* (2019) 'A Review on Coordination Properties of Thiol-Containing Chelating Agents Towards Mercury, Cadmium, and Lead', *Molecules*, 24(18), p. 3247. doi:10.3390/molecules24183247.

Bocquet, A. *et al.* (2021) 'Potential toxicity of metal trace elements from food in children', *Archives de Pédiatrie*, 28(3), pp. 173–177. doi:10.1016/j.arcped.2021.03.001.

Bourlieu, C. *et al.* (2014) 'Specificity of Infant Digestive Conditions: Some Clues for Developing Relevant In Vitro Models', *Critical Reviews in Food Science and Nutrition*, 54(11), pp. 1427–1457. doi:10.1080/10408398.2011.640757.

Brereton, R.G. (2014) 'The normal distribution', *Journal of Chemometrics*, 28(11), pp. 789–792. doi:10.1002/cem.2655.

Charis Galanakis (2017) *What is the Difference Between Bioavailability Bioaccessibility and Bioactivity of Food Components? | SciTech Connect*. Available at: https://scitechconnect.elsevier.com/bioavailability-bioaccessibility-bioactivity-food-components/ (Accessed: 15 May 2022).

Crans, D.C. *et al.* (2004) 'The chemistry and biochemistry of vanadium and the biological activities exerted by vanadium compounds', *Chemical Reviews*, 104(2), pp. 849–902. doi:10.1021/cr020607t.

Duffus, J. (2002) 'Heavy metals" a meaningless term? (IUPAC Technical Report)', *Pure and Applied Chemistry*, 74, pp. 793–807. doi:10.1351/pac200274050793.

(EC) No 1881/2006 (2006). Available at: https://eur-lex.europa.eu/eli/reg/2006/1881/oj (Accessed: 15 May 2022).

EFSA (ed.) (2006) *Tolerable upper intake levels for vitamins and minerals*. Parma: European Food Safety Authority.

Ejaz, A. *et al.* (2022) 'Assessment of cobalt in wheat grains as affected by diverse fertilizers: implications for public health', *Environmental Science and Pollution Research*, 29(23), pp. 34558–34574. doi:10.1007/s11356-022-18528-0.

Engwa, G.A. *et al.* (2019) *Mechanism and Health Effects of Heavy Metal Toxicity in Humans*, *Poisoning in the Modern World - New Tricks for an Old Dog?* IntechOpen. doi:10.5772/intechopen.82511.

Ewer, A.K. *et al.* (1994) 'Gastric emptying in preterm infants', *Archives of Disease in Childhood. Fetal and Neonatal Edition*, 71(1), pp. F24-27. doi:10.1136/fn.71.1.f24.

Guo, G. *et al.* (2018) 'Accumulation of As, Cd, and Pb in Sixteen Wheat Cultivars Grown in Contaminated Soils and Associated Health Risk Assessment', *International Journal of Environmental Research and Public Health*, 15(11). doi:10.3390/ijerph15112601.

Holland, H.D. (2014) *Treatise on geochemistry*. Amsterdam: Elsevier.

Ianiro, G. *et al.* (2016) 'Digestive Enzyme Supplementation in Gastrointestinal Diseases', *Current Drug Metabolism*, 17(2), pp. 187–193. doi:10.2174/1389200217021601141501 37.

Kasozi, K.I. *et al.* (2021) 'Descriptive Analysis of Heavy Metals Content of Beef From Eastern Uganda and Their Safety for Public Consumption', *Frontiers in Nutrition*, 8. Available at: https://www.frontiersin.org/article/10.3389/fnut.2021.592340 (Accessed: 26 May 2022).

Khan, A. *et al.* (2015) 'The uptake and bioaccumulation of heavy metals by food plants, their effects on plants nutrients, and associated health risk: a review', *Environmental Science and Pollution Research International*, 22(18), pp. 13772–13799. doi:10.1007/s11356-015-4881-0.

Liem-Nguyen, V. *et al.* (2020) 'Removal mechanism of arsenic (V) by stainless steel slags obtained from scrap metal recycling', *Journal of Environmental Chemical Engineering*, 8(4), p. 103833. doi:10.1016/j.jece.2020.103833.

Livsmedelsverket (2018) *Metaller i barnmat och ris*. Available at: https://www.livsmedelsverket.se/globalassets/publikationsdatabas/rapporter/2018/2018-nr-19-metaller-i-barnmat-och-ris.pdf (Accessed: 29 January 2022).

Luan Gjokaj (2017) *Barnmatsmarknaden värd 1,5 miljard "Vi fyller ekologiskt tomrum"*, *Investerarbrevet*. Available at: https://investerarbrevet.se/barnmatsmarknaden-vard-15-miljard-vi-fyller-ekologiskt-tomrum/ (Accessed: 16 May 2022).

Luch, A. (ed.) (2010) *Clinical Toxicology*. Basel Boston Berlin: Birkhäuser (Molecular, Clinical and Environmental Toxicology, 2).

Ménard, O. *et al.* (2018) 'A first step towards a consensus static in vitro model for simulating full-term infant digestion', *Food Chemistry*, 240, pp. 338–345. doi:10.1016/j.foodchem.2017.07.145.

Nimpuno, N. *et al.* (2011) *Information on chemicals in electronic products: a study of needs, gaps, obstacles and solutions to provide and access information on chemicals in electronic products*. Copenhagen: Nordic Council of Ministers : Nordic Council.

Petrucci, R.H. *et al.* (2017) *General chemistry: principles and modern applications*. Tenth edition. Upper Saddle River, N.J: Pearson Canada Inc.

Rehder, D. (2013) 'Vanadium. Its role for humans', *Metal Ions in Life Sciences*, 13, pp. 139–169. doi:10.1007/978-94-007-7500-8_5.

Reimer, J. (2012) *From Altair to iPad: 35 years of personal computer market share*, *Ars Technica*. Available at: https://arstechnica.com/information-technology/2012/08/from-altair-to-ipad-35-years-of-personal-computer-market-share/ (Accessed: 26 May 2022).

Russ Rowlett (2018) *USP unit*, *https://www.ibiblio.org/units/dictU.html*. Available at: https://www.ibiblio.org/units/dictU.html (Accessed: 15 May 2022).

Shahzad, B. *et al.* (2016) 'Lithium toxicity in plants: Reasons, mechanisms and remediation possibilities – A review', *Plant Physiology and Biochemistry*, 107, pp. 104–115. doi:10.1016/j.plaphy.2016.05.034.

Sóvágó, I. and Várnagy, K. (2013) 'Cadmium(II) complexes of amino acids and peptides', *Metal Ions in Life Sciences*, 11, pp. 275–302. doi:10.1007/978-94-007-5179-8_9.

WHO (2006) *Length/height-for-age, weight-for-age, weight-for-length, weight-for-height and body mass index-for-age; methods and development*. Edited by M. de Onis. Geneva: WHO Press (WHO child growth standards).

7. ACKNOWLEDGMENTS

I would like to thank my supervisor Michaela Zeiner for encouraging me and giving me support and direction when I needed it the most.

I would also like to thank my friends and family, especially my wife Katarina for carrying such a heavy burden to make it possible for me to finish this project.

And finally I want to thank my daughter Alice who always was able to put a smile on my face when nothing else could.

APPENDIX

ICP-MS Merck VI multi element standard solution calibration

Table 1. ICP-MS calibration standard concentrations γ [µg L^{-1}]. Date: 220309

Standard	Standard γ [µg L^{-1}]	^{7}Li	^{51}V	^{59}Co	^{60}Ni	^{75}As	^{82}Se	^{111}Cd	^{208}Pb
ST0A.D	0	<0.10	0	0	0	<0.01	<0.97	0	<0.01
ST001A.D	0.01	<0.10	0.0111	0.0106	0.0143	0.110	<0.97	0.0105	0.0114
ST01A.D	0.1	0.0972	0.0968	0.102	0.0976	0.940	0.991	0.105	0.102
ST1A.D	1	0.980	0.964	1.02	1.00	9.73	9.83	0.970	0.983
ST10A.D	10	9.94	9.82	10.2	9.88	97.1	101	9.89	9.76
ST100A.D	100	100	100	100	100	1000	1000	100	100

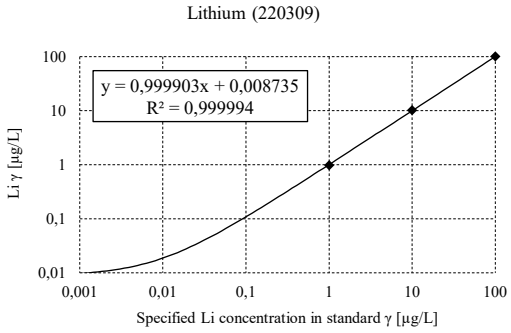

Figure 1. ICP-MS calibration curve for lithium in Merck VI standard solution. Date: 220309

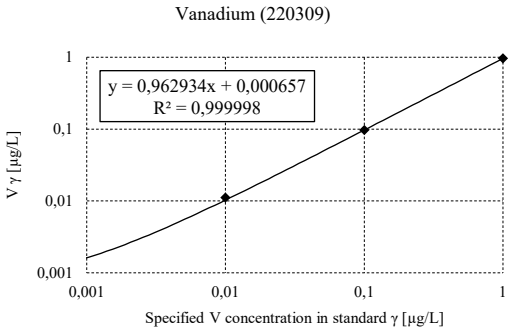

Figure 2. ICP-MS calibration curve for vanadium in Merck VI standard solution. Date: 220309

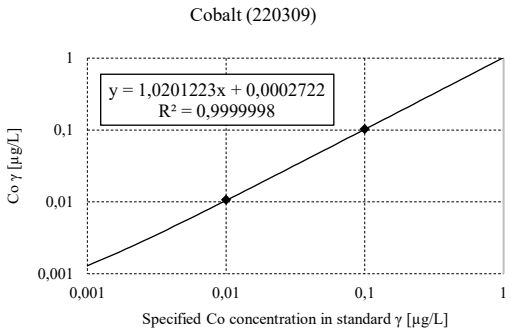

Figure 3. ICP-MS calibration curve for cobalt in Merck VI standard solution. Date: 220309

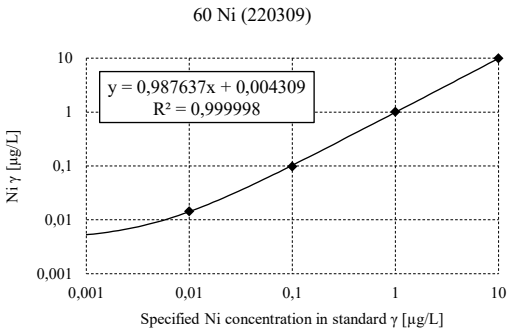

Figure 4. ICP-MS calibration curve for nickel in Merck VI standard solution. Date: 220309

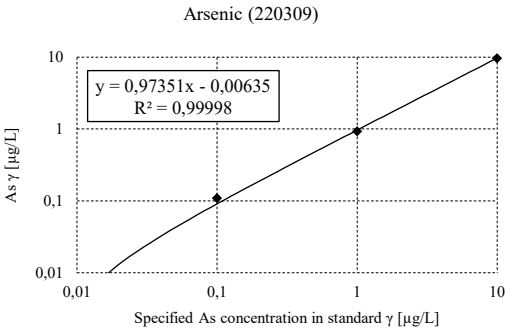

Figure 5. ICP-MS calibration curve for arsenic in Merck VI standard solution. Date: 220309

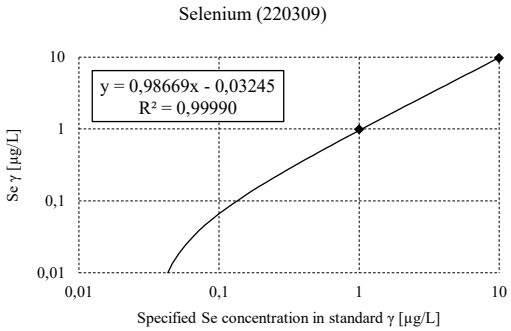

Figure 6. ICP-MS calibration curve for selenium in Merck VI standard solution. Date: 220309

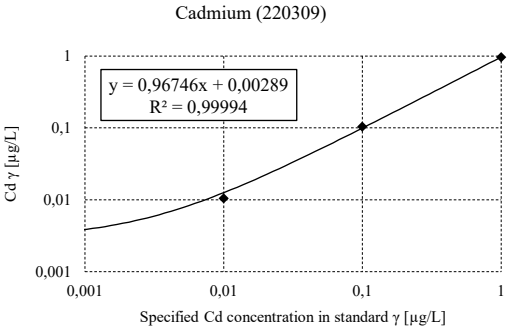

Figure 7. ICP-MS calibration curve for cadmium in Merck VI standard solution. Date: 220309

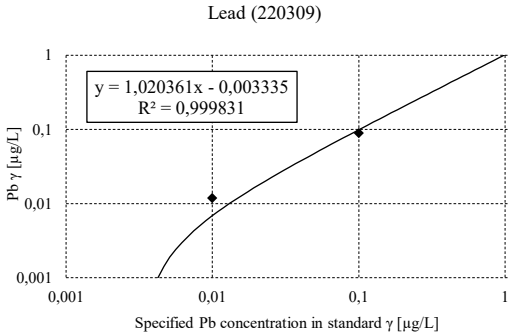

Figure 8. ICP-MS calibration curve for lead in Merck VI standard solution. Date: 220309